Electronic Supplementary Information

Chirality transcription in the anion-coordination-driven assembly of tetrahedral cages

Jin Fu,[#a] Bo Zheng,[#a] Huizheng Zhang,[a] Yanxia Zhao,[a] Dan Zhang,[a] Wenyao Zhang,[a] Xiao-Juan Yang[a] and Biao Wu*[a,b]

[a] *Key Laboratory of Synthetic and Natural Functional Molecule Chemistry of the Ministry of Education, College of Chemistry and Materials Science, Northwest University, Xi'an 710127, China. E-mail: wubiao@nwu.edu.cn*

[b] *State Key Laboratory of Applied Organic Chemistry, Lanzhou University, Lanzhou 730000, China*

Table of Contents:

S1. General considerations

o-Nitro-phenylisocyanate, (R)-(+)-1-phenylethyl isocyanate, (S)-(−)-1-phenylethyl isocyanate, benzyl isocyanate were purchased from Alfa Aesar and used as received. 4-Nitrophenyl chloroformate, (R)-2-phenyl-1-propylamine and (S)-2-phenyl-1-propylamine were purchased from TCI and used as received. All solvents and other reagents were of reagent grade quality and purchased commercially. ^{1}H NMR, COSY, DOSY and ^{13}C NMR spectra were recorded on a Bruker AVANCE III-400 spectrometer at 400, 100 MHz, respectively (^{1}H NMR: 2.50 ppm for DMSO-d_6, 2.05 ppm for acetone-d_6 and 1.94 ppm for CD_3CN respectively; ^{13}C NMR: 39.6 ppm for DMSO-d_6). Mass spectra were performed with a Bruker microTOF-Q II ESI-Q-TOF LC/MS/MS instrument. Single crystal diffraction analyses were done on a Bruker D8 Venture photon II diffractometer. Circular dichroism (CD) spectra were performed with JEOL J-1500, using a 1 cm quartz cuvette.

S2. Synthesis of ligands

Compounds **TAPA**, **A**, **B** and **C** were synthesized according to literature procedures.[1,2]

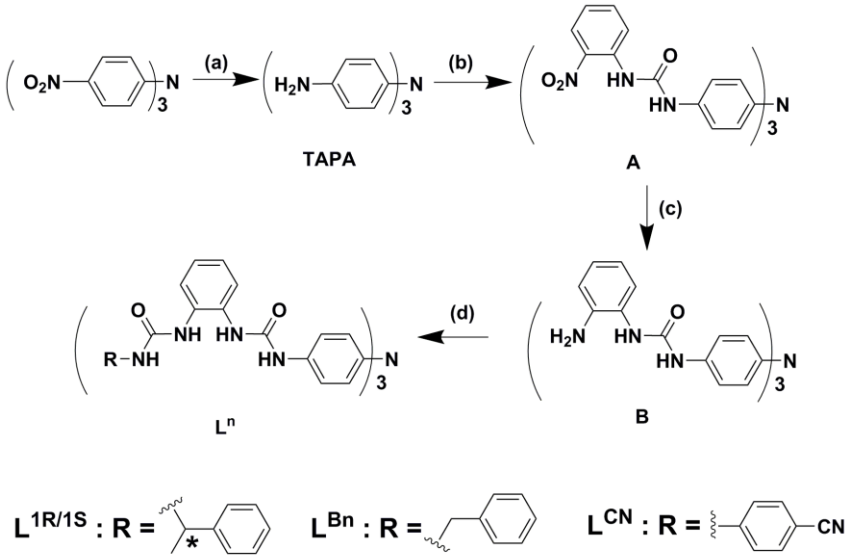

Scheme S1. Synthesis of the ligand $\mathbf{L^n}$ (a) $NH_2NH_2 \cdot H_2O$, Pd/C 10% cat., ethanol, reflux, 84%; (b) *o*-Nitro-phenylisocyanate, THF, reflux, 93%; (c) $NH_2NH_2 \cdot H_2O$, Pd/C 10% cat., ethanol, reflux, 80%; (d) (R)-(+)-1-Phenylethyl isocyanate, DMF, r.t., 85%; (S)-(−)-1-phenylethyl isocyanate, DMF, r.t., 79%; Benzyl isocyanate, DMF, r.t., 79%; 4-cyanophenyl isocyanate, THF/DMF, reflux, 54%.

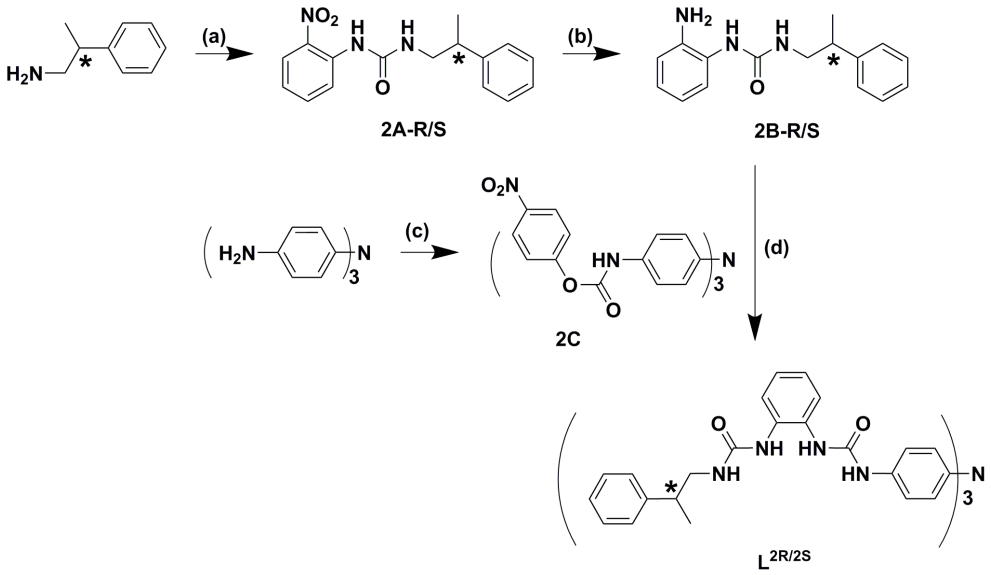

Scheme S2. Synthesis of the ligand $\mathbf{L}^{2R/2S}$ (a) *o*-Nitro-phenylisocyanate, THF, reflux, 96%; (b) NH_2NH_2 ·H_2O, Pd/C 10% cat., ethanol, reflux, 57%; (c). 4-Nitrophenyl chloroformate, THF, reflux, 83%; (d) 2B+2C, triethylamine, THF, reflux, 87%.

Compound TAPA: ^{1}H NMR (400 MHz, DMSO-d_6, ppm): δ 6.58 (d, 1H, H2), 6.44 (d, 1H, H1), 4.69 (s, 1H, Ha).

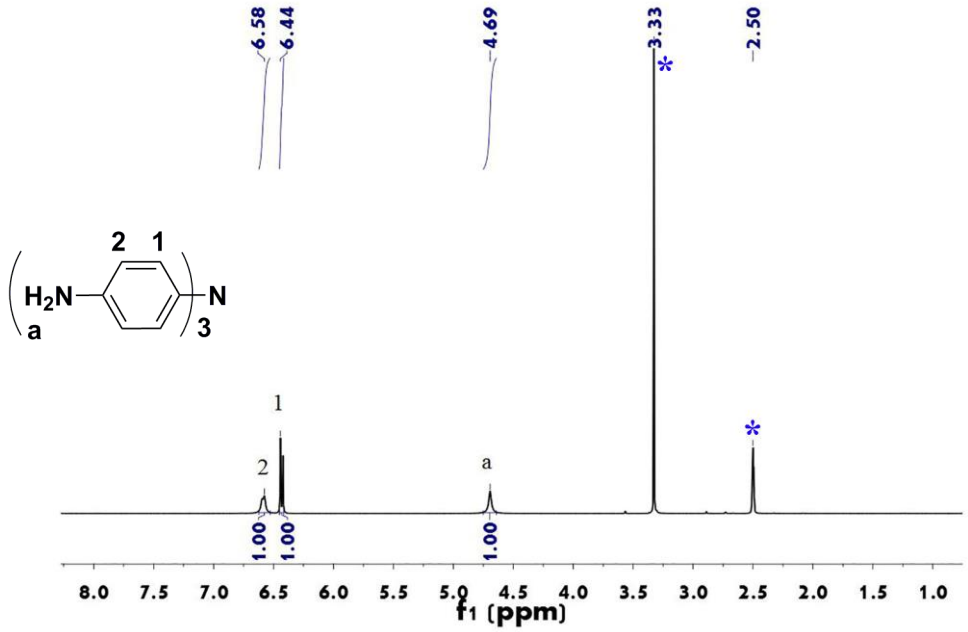

Fig. S1. ^{1}H NMR spectrum of compound **TAPA** (400 MHz, DMSO-d_6, 298 K).

Compound A: ^{1}H NMR (400 MHz, DMSO-d_6, ppm): δ 9.79 (s, 1H, NHb), 9.58 (s, 1H, NHa), 8.31 (d, 1H, H6), 8.10-8.08 (dd, 1H, H3), 7.72-7.67 (m, 1H, H4), 7.40 (d, 2H, H2), 7.21-7.17 (m, 1H, H5), 6.97 (d, 1H, H1).

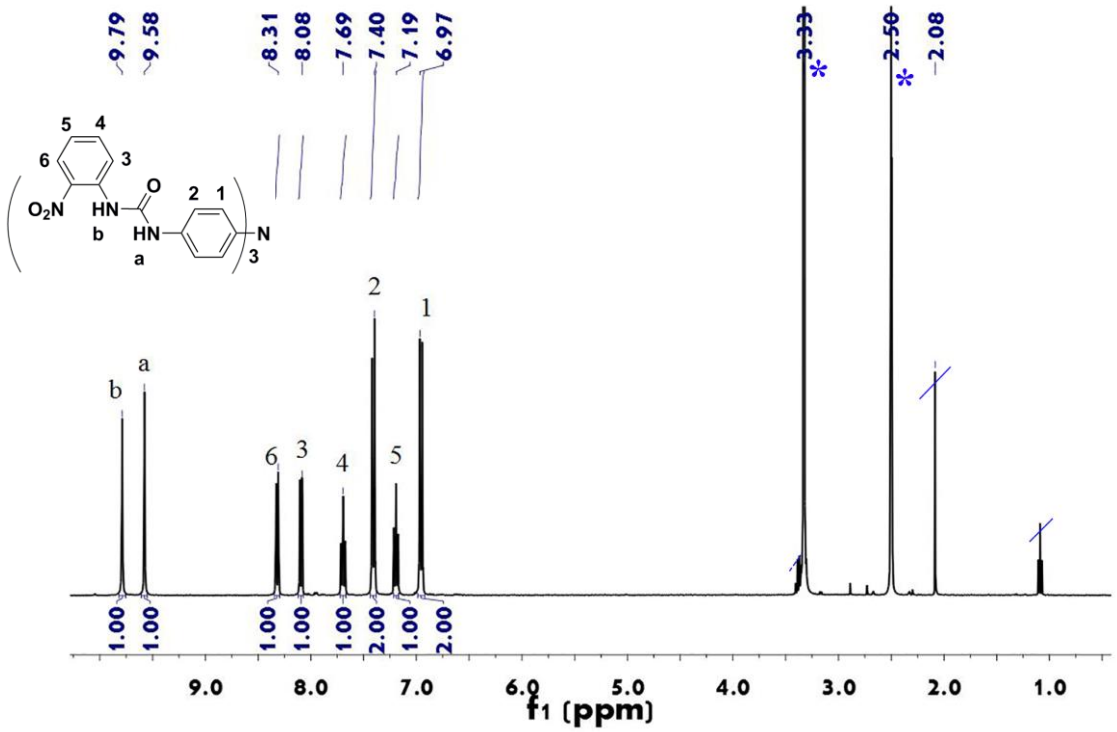

Fig. S2. ^{1}H NMR spectrum of compound **A** (400 MHz, DMSO-d_6, 298 K).

Compound B: ^{1}H NMR (400 MHz, DMSO-d_6, ppm): δ 8.66 (s, 1H, NHb) , 7.67 (s, 1H, NHa), 7,33 (d, 3H, H2/3), 6.91 (d, 2H, H1), 6.83 (t, 1H, H5), 6.74 (d, 1H, H4), 6.57 (t, 1H, H6), 4.76 (s, 2H, NHc).

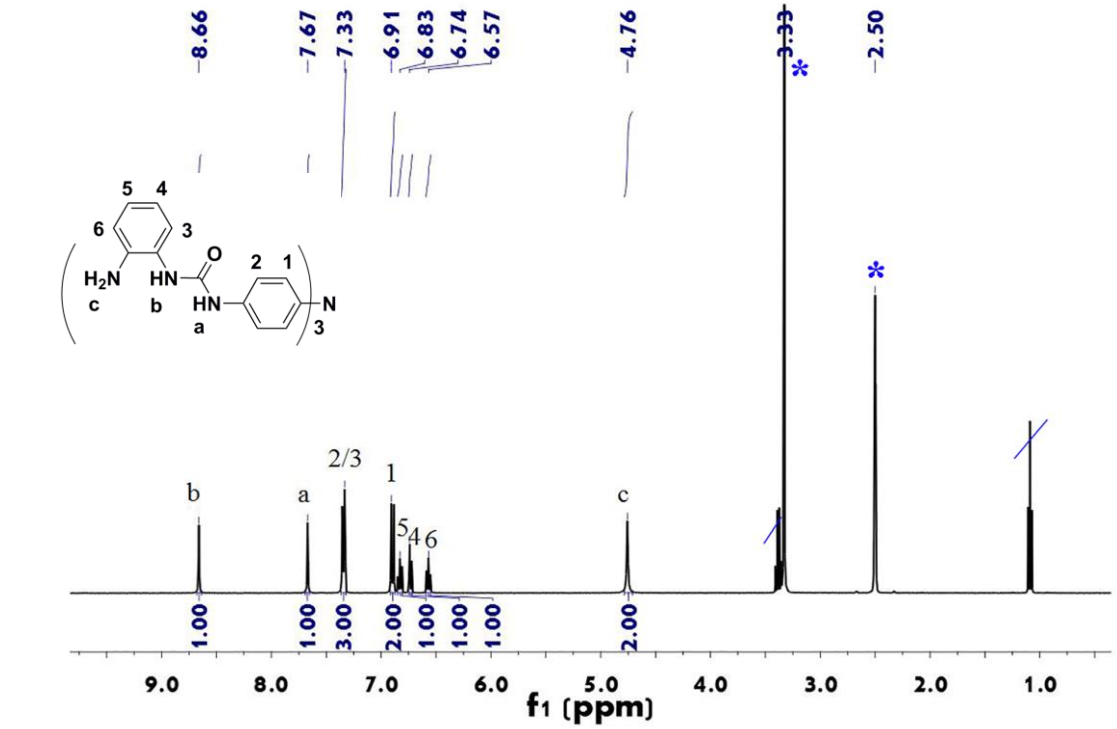

Fig. S3. ^{1}H NMR spectrum of compound **B** (400 MHz, DMSO-d_6, 298 K).

Ligand L^{1R}:

(R)-(+)-1-phenylethyl isocyanate (0.11 g, 0.73 mmol) was added to a DMF solution (1 mL) of compound **B** (0.10 g, 0.15 mmol). After stirring intensely overnight, the precipitate was filtered off, washed with diethyl ether and then dried over in vacuum to yield $\mathbf{L^{1R}}$ as a brown solid (0.14 g, 85%). ^{1}H NMR (400 MHz, DMSO-d_6, ppm): δ 8.92 (s, 1H, NHa), 7.92 (s, 1H, NHb), 7.83 (s, 1H, NHc), 7.57 (d, J = 8 Hz, 1H, H3), 7.45 (d, J = 8 Hz, 1H, H6), 7.34 (m, 6H, H2/9/10), 7.22 (m, 1H, H11), 7.00 (m, 3H, H4/5/NHd), 6.91 (d, J = 8 Hz, 2H, H1), 4.84 (m, 1H, H7), 1.40 (d, J = 8 Hz, 9H, H8). ^{13}C NMR (100 MHz, DMSO-d_6, ppm): 155.1, 153.4, 145.2, 142.1, 134.8, 132.8, 130.1, 128.4, 126.7, 126.0, 124.7, 124.2, 123.8, 123.0, 122.7, 119.7, 48.9, 23.1. ESI-MS: m/z 1156.4495, $[M+Na]^+$.

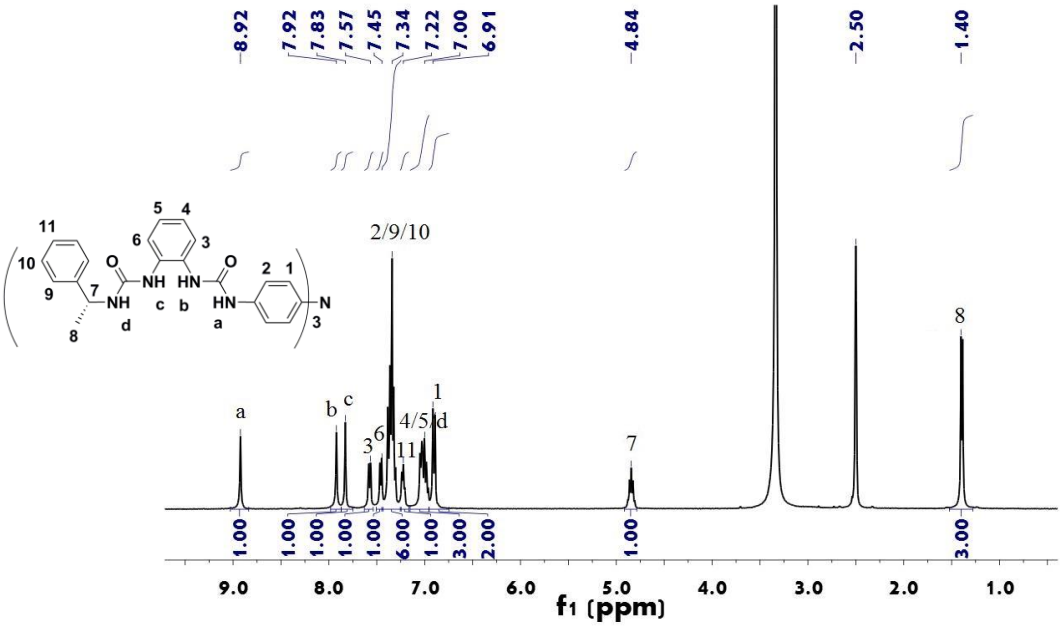

Fig. S4. ^{1}H NMR spectrum of $\mathbf{L^{1R}}$ (400 MHz, DMSO-d_6, 298 K).

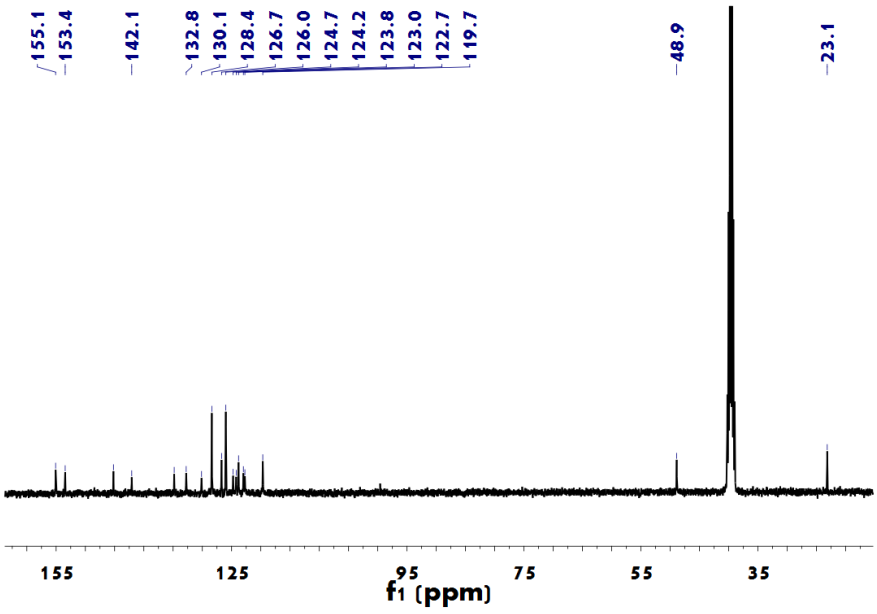

Fig. S5. ^{13}C NMR spectrum of $\mathbf{L^{1R}}$ (100 MHz, DMSO-d_6, 298 K).

Ligand L^{1S}:

(S)-(−)-1-phenylethyl isocyanate (0.11 g, 0.73 mmol) was added to a DMF solution (1 mL) of compound **B** (0.10 g, 0.15 mmol). After stirring intensely overnight, the precipitate was filtered off, washed with diethyl ether and then dried over in vacuum to yield $\mathbf{L^{1S}}$ as a brown solid (0.13 g, 79%). ^{1}H NMR (400 MHz, DMSO-d_6, ppm): δ 8.93 (s, 1H, NHa), 7.93 (s, 1H, NHb), 7.83 (s, 1H, NHc), 7.57 (d, J = 8 Hz, 1H, H3), 7.45 (d, J = 8 Hz, 1H, H6), 7.34 (m, 6H, H2/9/10), 7.22 (m, 3H, H11), 7.00 (m, 9H, H4/5/NHd), 6.91 (d, J = 8 Hz, 2H, H1), 4.84 (m, 1H, H7), 1.40 (d, J = 8 Hz, 1H, H8). ^{13}C NMR (100 MHz, DMSO-d_6, ppm):155.1, 153.5, 145.2, 142.1, 134.8, 132.8, 130.1, 128.4, 126.7, 126.0, 124.7, 124.2, 123.8, 123.0, 122.7, 119.7, 48.9, 23.2. ESI-MS: m/z 1156.4551, $[M+Na]^+$.

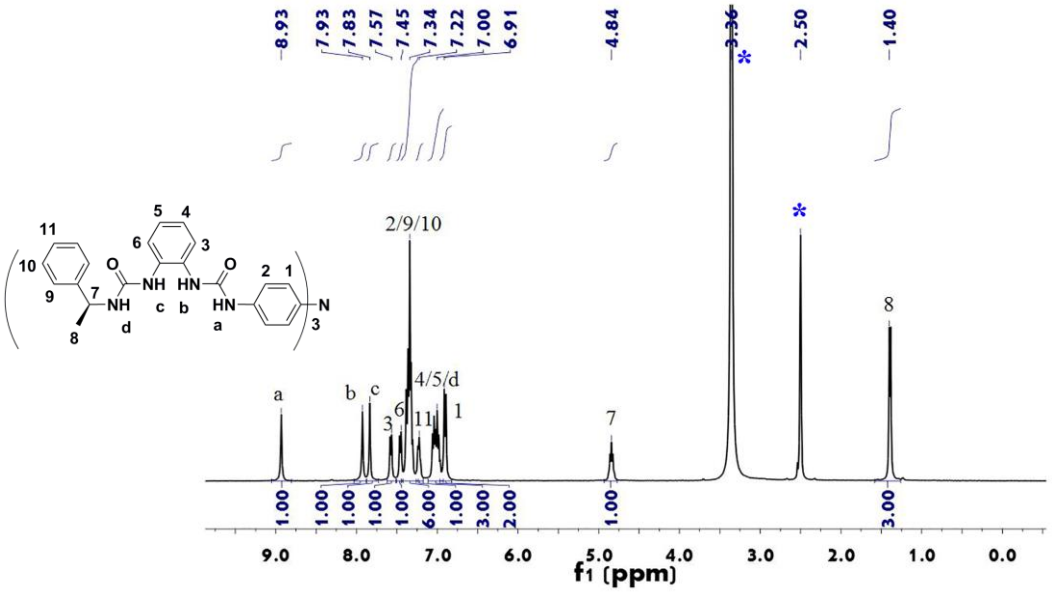

Fig. S6. ^{1}H NMR spectrum of $\mathbf{L^{1S}}$ (400 MHz, DMSO-d_6, 298 K).

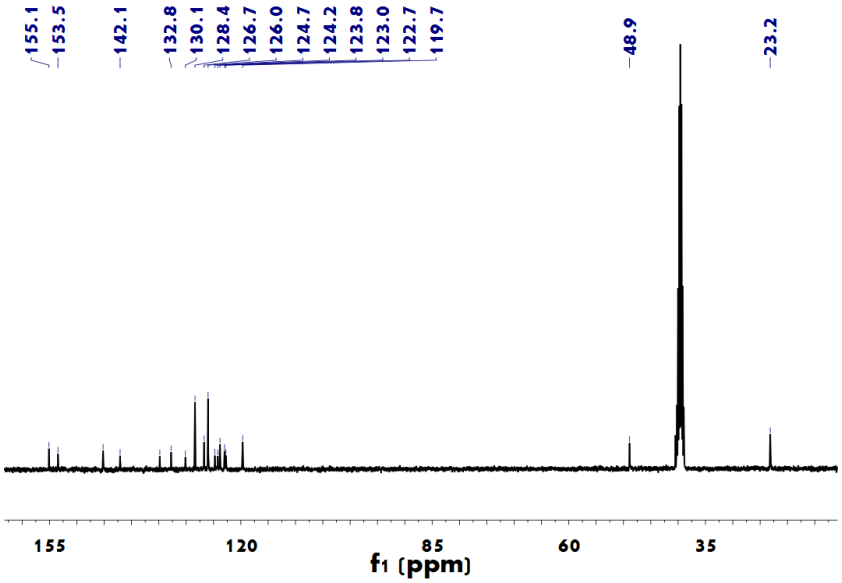

Fig. S7. ^{13}C NMR spectrum of $\mathbf{L^{1S}}$ (100 MHz, DMSO-d_6, 298 K).

Ligand L^{Bn}:

Benzyl isocyanate (0.11 g, 0.80 mmol) was added to a DMF solution (1 mL) of compound **B** (0.10 g, 0.15 mmol). After stirring intensely overnight, the precipitate was filtered off by diethyl ether and then dried over in vacuum to yield $\mathbf{L^{Bn}}$ as a gray solid (0.15 g, 79%). ^{1}H NMR (400 MHz, DMSO-d_6, ppm): δ 9.00 (s, 1H, NHa), 7.98 (s, 1H, NHb), 7.93 (s, 1H, NHc), 7.54 (m, 2H, H3/6), 7.36 (d, J = 8 Hz, 2H, H2), 7.31 (d, J = 8 Hz, 4H, H8/9), 7.24 (m, 1H, H10), 7.03 (m, 2H, H4/5), 6.99 (m, 1H, NHd), 6.89 (d, J = 8 Hz, 2H, H1), 4.30 (d, J = 8 Hz, 2H, H7). ^{13}C NMR (100 MHz, DMSO-d_6, ppm): 156.1, 153.3, 142.1, 140.3, 134.8, 132.0, 131.2, 128.4, 127.4, 126.8, 124.1, 124.0, 123.8, 123.7, 123.6, 119.7, 43.1. ESI-MS: m/z 1114.9325, $[M+Na]^+$.

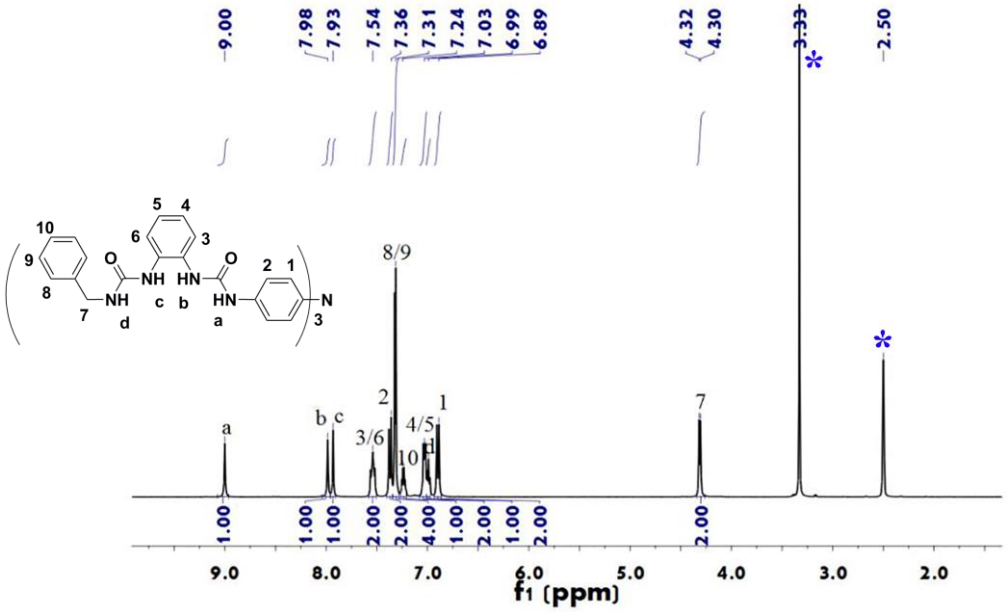

Fig. S8. ^{1}H NMR spectrum of $\mathbf{L^{Bn}}$ (400 MHz, DMSO-d_6, 298 K).

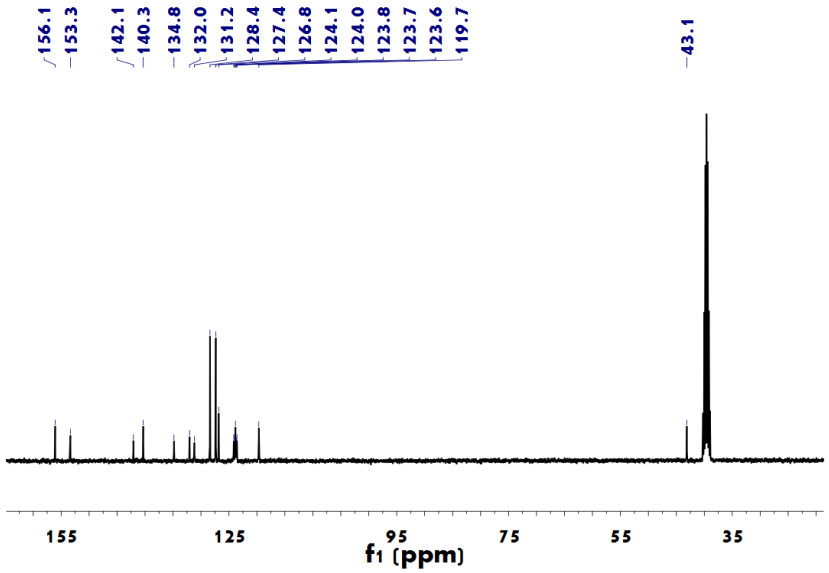

Fig. S9. ^{13}C NMR spectrum of $\mathbf{L^{Bn}}$ (100 MHz, DMSO-d_6, 298 K).

Ligand L^{CN}:

To a THF solution (50 mL) of 4-cyanophenyl isocyanate (0.21 g, 1.46 mmol) was added to a DMF solution (1 mL) of compound **B** (0.20 g, 0.30 mmol). After refluxing under intensely stirring overnight, the precipitate was filtered off, washed with diethyl ether and then dried over in vacuum to yield $\mathbf{L}^{CN}$ as a gray solid (0.18 g, 54%). ^{1}H NMR (400 MHz, DMSO-d_6, ppm): δ 9.61 (s, 3H, NHd), 9.00 (s, 3H, NHc), 8.21 (s, 3H, NHb), 8.05 (s, 3H, NHa), 7.72 (d, J = 8 Hz, 6H, H8), 7.68 (m, 9H, H7/6), 7.53 (d, J = 8 Hz,3H, H3), 7.37 (d, J = 8 Hz, 6H, H2), 7.15-7.07 (m, 6H, H4/5), 6.93 (d, J = 8 Hz, 6H, H1). ^{13}C NMR (100 MHz, DMSO-d_6, ppm): 153.3, 153.0, 144.5, 142.2, 134.6, 133.4, 132.3, 130.3, 125.0, 124.9, 123.9, 123.6, 119.8, 119.4, 118.1, 103.3. ESI-MS: m/z 1147.8760, $[M+Na]^+$.

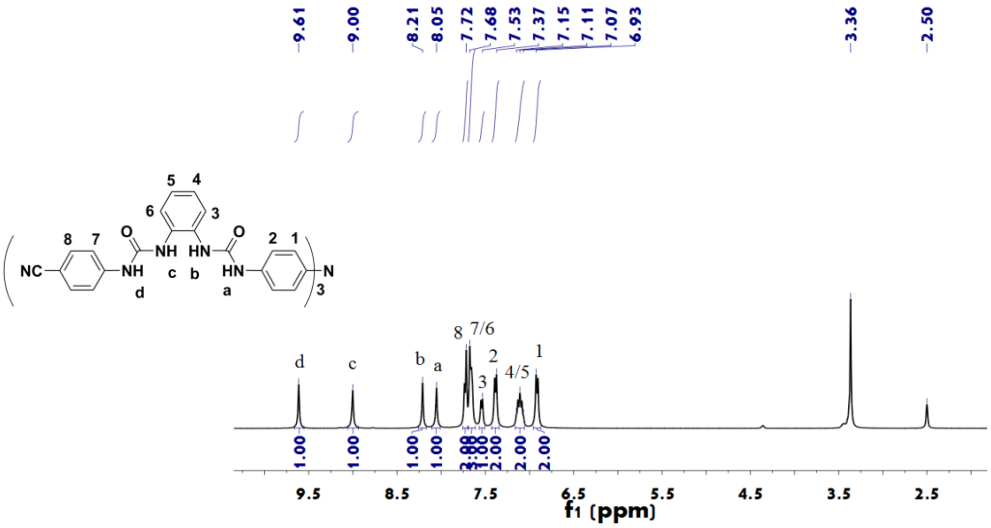

Fig. S10. ^{1}H NMR spectrum of $\mathbf{L}^{CN}$ (400 MHz, DMSO-d_6, 298 K).

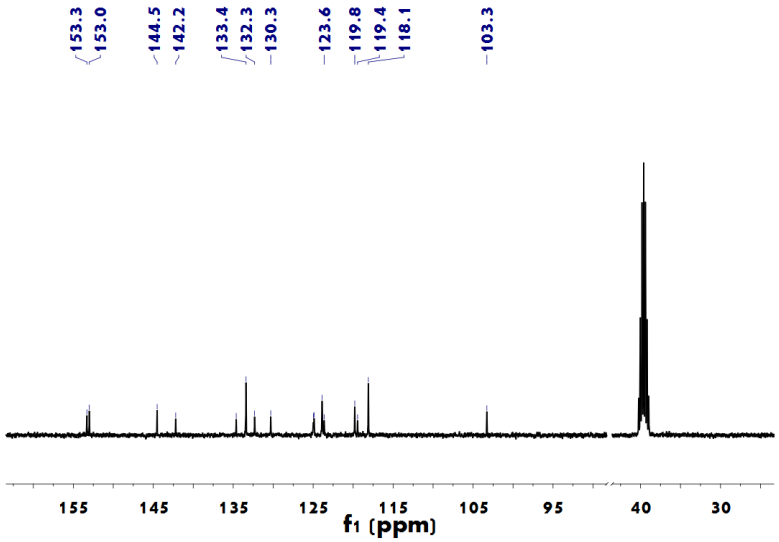

Fig. S11. ^{13}C NMR spectrum of $\mathbf{L}^{CN}$ (100 MHz, DMSO-d_6, 298 K).

Compound 2C:

To a THF solution (80 mL) of 4-nitrophenyl chloroformate (0.81 g, 4.00 mmol) was added a THF solution (15 mL) of compound **TAPA** (0.29 g, 1.00 mmol). After refluxing under intensely stirring for 6 h, the precipitate was filtered off, washed several times with diethyl ether and then dried over in vacuum to yield **2C** as an orange solid (0.65 g, 83%). ^{1}H NMR (400 MHz, DMSO-d_6, ppm): δ 10.42 (s, 1H, NHa), 8.30 (d, J = 8 Hz, 2H, H4), 7.54 (d, J = 8 Hz, 2H, H3), 7.42 (d, J = 8 Hz, 6H, H2), 6.99 (d, J = 8 Hz, 6H, H1). ^{13}C NMR (100 MHz, DMSO-d_6, ppm): 155.8, 150.7, 144.6, 143.1, 133.0, 125.4, 124.1, 122.9, 120.3. ESI-MS: m/z 824.5832, $[M+K]^+$.

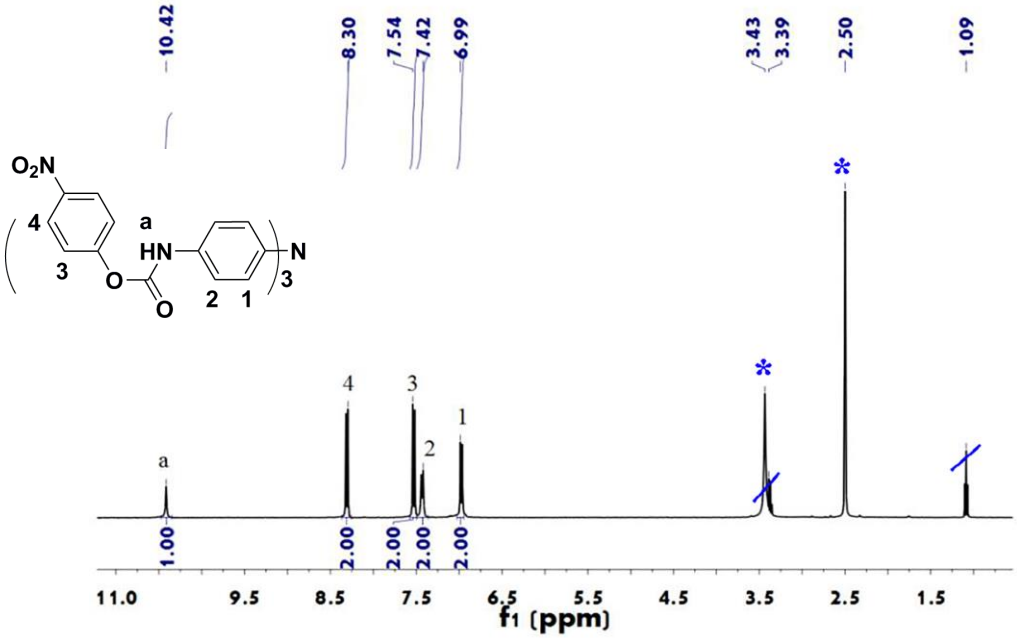

Fig. S12. ^{1}H NMR spectrum of compound **2C** (400 MHz, DMSO-d_6, 298 K).

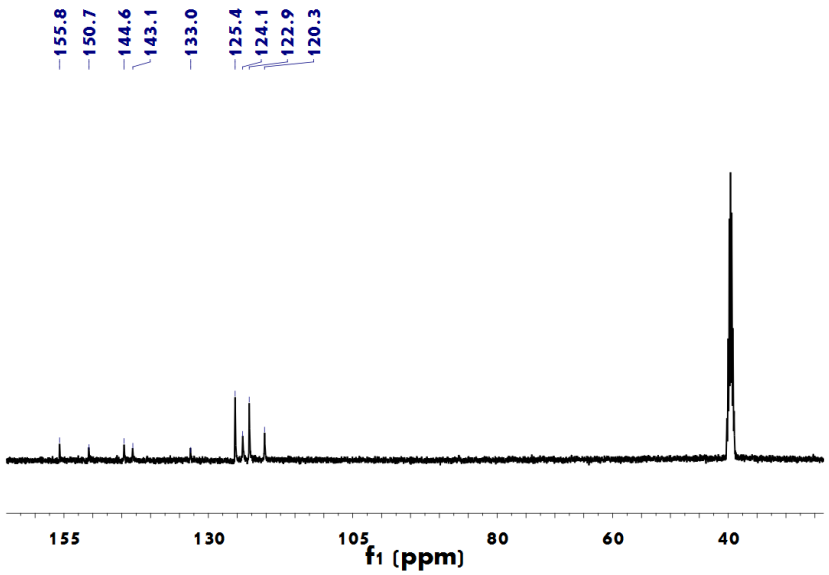

Fig. S13. ^{13}C NMR spectrum of compound **2C** (100 MHz, DMSO-d_6, 298 K).

Compound 2A-R:

To a THF solution (5 mL) of *o*-nitro-phenylisocyanate (0.66 g, 4.00 mmol) was added (R)-2-phenyl-1-propylamine (580 μL, 0.54 g, 4.00 mmol). After under intensely stirring at room temperature overnight, the precipitate was filtered off, washed several times with diethyl ether and then dried over in vacuum to yield **2A-R** as an orange solid (1.15 g, 96%). ^{1}H NMR (400 MHz, DMSO-d_6, ppm): δ 9.30 (s, 1H, NHb), 8.27 (d, J = 8 Hz, 1H, H10), 8.02 (d, J = 8 Hz, 1H, H7), 7.62 (m, 1H, H8), 7.50 (t, 1H, NHa), 7.32 (m, 2H, H2), 7.27 (m, 2H, H3), 7.21 (m, 2H, H9), 7.10 (m, 2H, H1), 3.28 (t, 2H, H6), 2.92 (m, 1H, H4), 1.22 (d, J = 4 Hz, 3H, H5). ^{13}C NMR (100 MHz, DMSO-d_6, ppm): 154.3, 144.8, 137.0, 135.9, 135.0, 128.5, 127.2, 126.3, 125.3, 122.2, 121.4, 46.4, 19.5. ESI-MS: m/z 322.3619, $[M+Na]^+$.

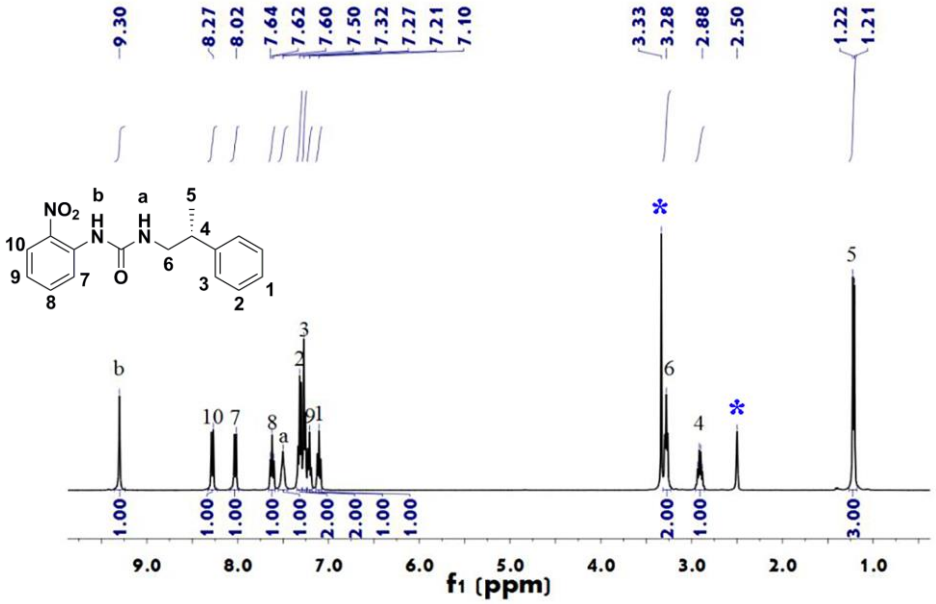

Fig. S14. ^{1}H NMR spectrum of compound **2A-R** (400 MHz, DMSO-d_6, 298 K).

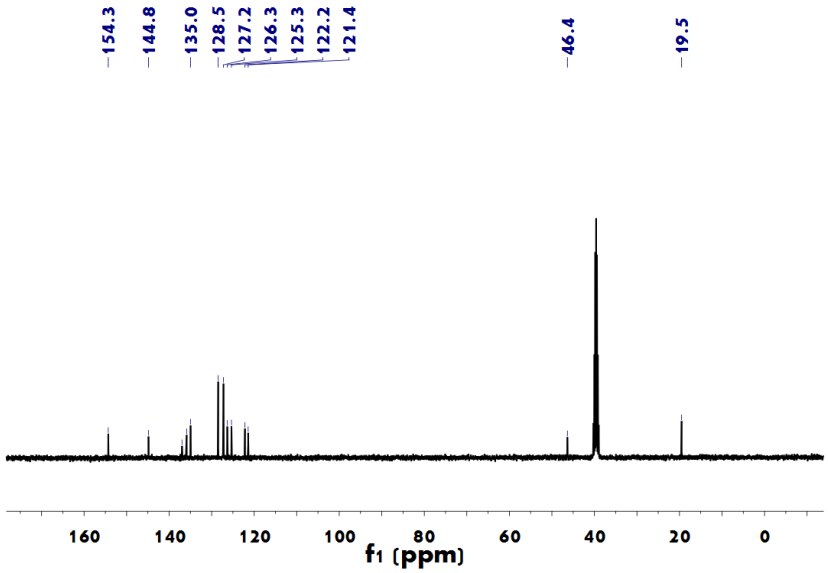

Fig. S15. ^{13}C NMR spectrum of compound **2A-R** (100 MHz, DMSO-d_6, 298 K).

Compound 2B-R:

Hydrazine monohydrate (25.0 mL) was added dropwise to a suspension of **2A-R** (1.60 g, 5.34 mmol) and Pd/C 10% (0.16 g, cat.) in ethanol (85 mL). After refluxing under stirring for 4 h, the solid was filtered through Celite to remove Pd/C. After the removal of most solvent, the resulting solution was poured into water (50 mL) and the precipitates thus formed was filtered off, washed several times with diethyl ether and dried over in vacuum to give a white solid **2B-R** (0.80 g, 57%). ^{1}H NMR (400 MHz, DMSO-d_6, ppm): δ 7.53 (s, 1H, NHb), 7.32 (m, 2H, H2), 7.27 (m, 4H, H3/7/9), 6.78 (m, 1H, H8), 6.69 (m, 1H, H1), 6.06 (m, 1H, NHa), 4.64 (s, 2H, Hc), 3.27 (m, 2H, H6), 2.88 (m, 1H, H4), 1.21 (d, J = 4 Hz, 3H, H5). ^{13}C NMR (100 MHz, DMSO-d_6, ppm): 155.9, 145.0, 140.5, 128.5, 127.3, 126.3, 125.6, 123.9, 123.3, 116.8, 115.8, 46.3, 39.8, 19.4. ESI-MS: m/z 292.1420, $[M+Na]^+$.

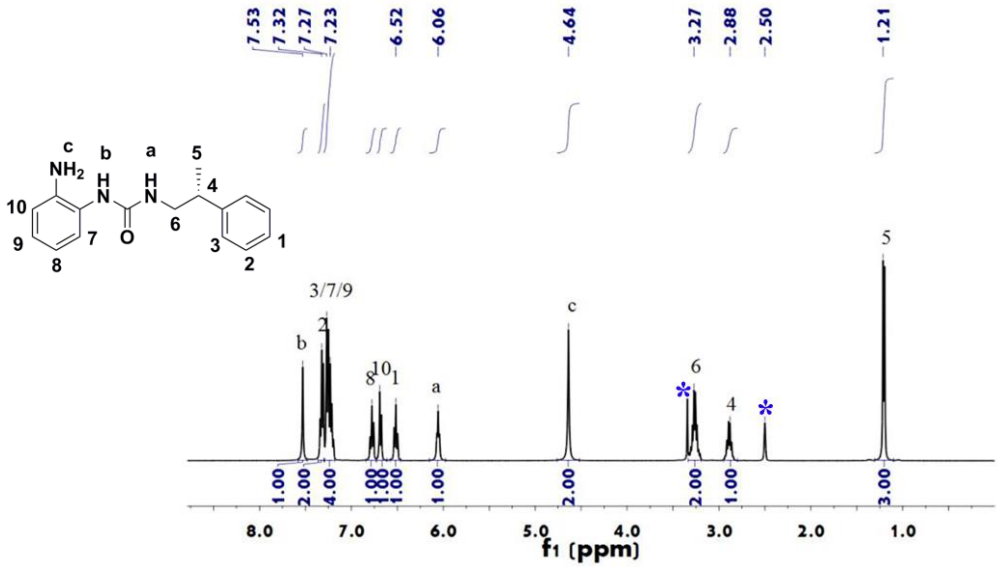

Fig. S16. ^{1}H NMR spectrum of compound **2B-R** (400 MHz, DMSO-d_6, 298 K).

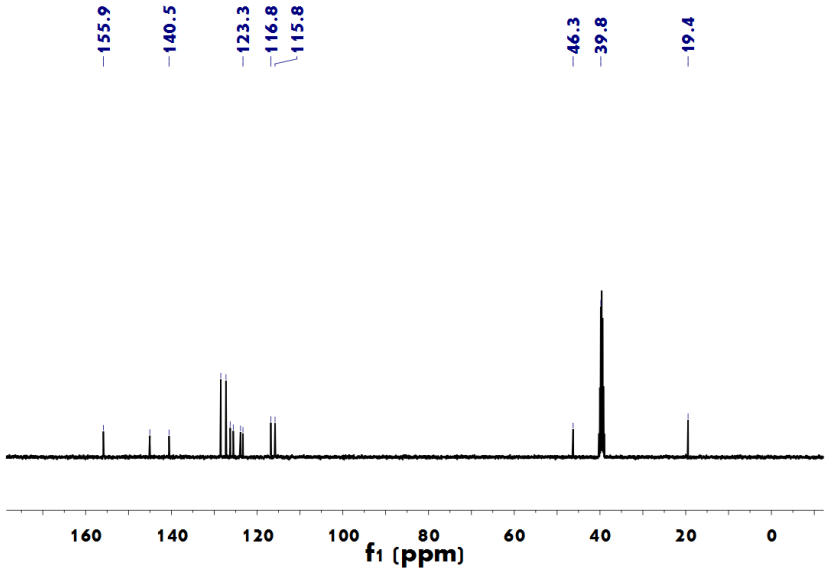

Fig. S17. ^{13}C NMR spectrum of compound **2B-R** (100 MHz, DMSO-d_6, 298 K).

Ligand L^{2R}:

Compound **2C** (0.10 g, 0.13 mmol) was dissolved in 10 mL THF and the solution was added dropwise into a 10 mL THF solution of **2B-R** (0.12 g, 0.43 mmol) and trimethylamine (200 μL). The mixture was refluxed overnight and the precipitate thus obtained was filtered off and washed with diethyl ether. After dried over in vacuum, a grey white solid $\mathbf{L^{2R}}$ (0.13 g, 87%) was obtained. ^{1}H NMR (400 MHz, DMSO-d_6, ppm): δ 8.99 (s, 1H, NHa), 7.94 (s, 1H, NHb), 7.86 (s, 1H, NHc), 7.53 (m, 1H, H3), 7.44 (m, 1H, H6), 7.34 (d, J = 8 Hz, 2H, H2), 7.30 (m, 1H, H11), 7.26 (d, J = 8 Hz, 2H, H10), 7.19 (m, 1H, H12), 6.91 (d, J = 8 Hz, 2H, H1), 6.42 (m, 1H, NHd), 3.27 (m, 6H, H7), 2.90 (m, 3H, H8), 1.21 (d, J = 8 Hz, 9H, H9). ^{13}C NMR (100 MHz, DMSO-d_6, ppm): 156.1, 153.3, 145.1, 142.1, 134.9, 132.0, 131.2, 128.6, 127.3, 126.4, 124.2, 123.9, 123.5, 119.7, 46.4, 39.4, 19.6. ESI-MS: m/z 1176.5566, $[M+H]^+$.

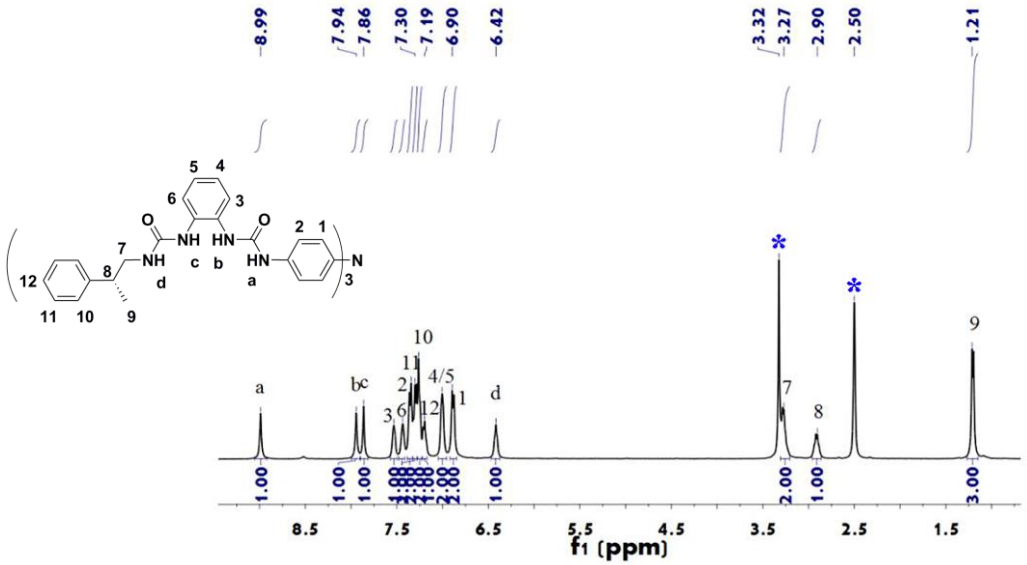

Fig. S18. ^{1}H NMR spectrum of $\mathbf{L^{2R}}$ (400 MHz, DMSO-d_6, 298 K).

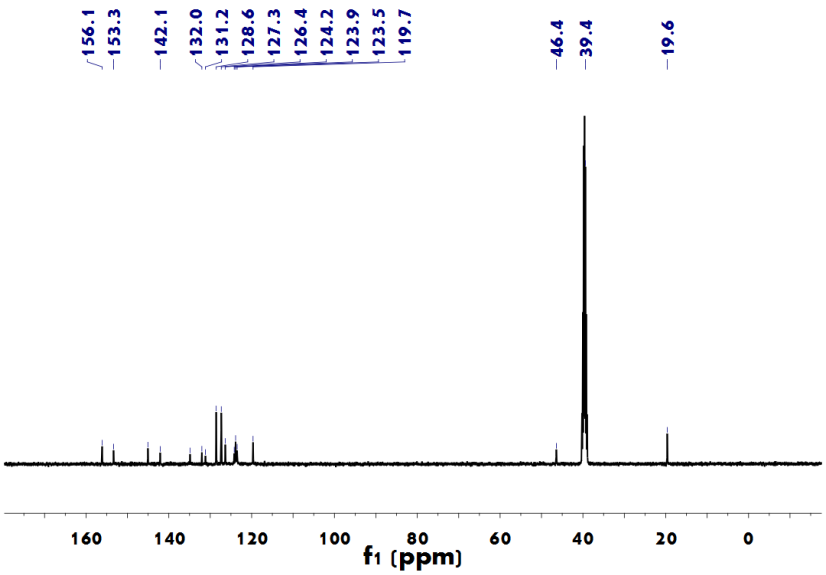

Fig. S19. ^{13}C NMR spectrum of $\mathbf{L^{2R}}$ (100 MHz, DMSO-d_6, 298 K).

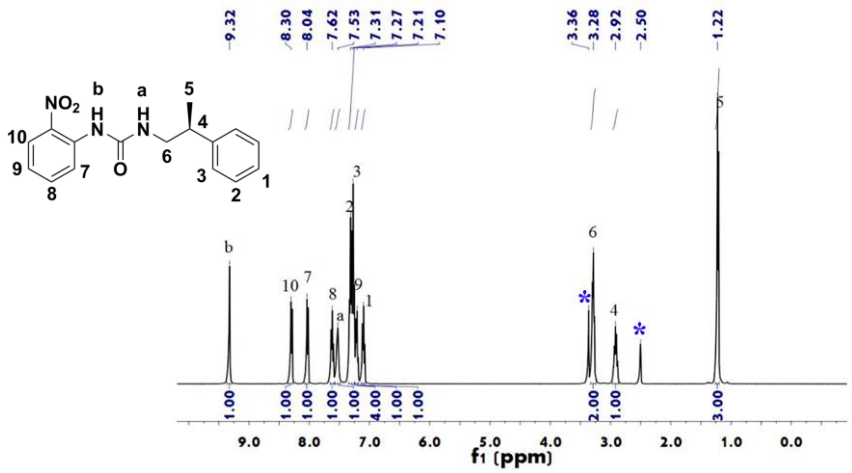

Fig. S20. [1]H NMR spectrum of compound **2A-S** (400 MHz, DMSO-d_6, 298 K).

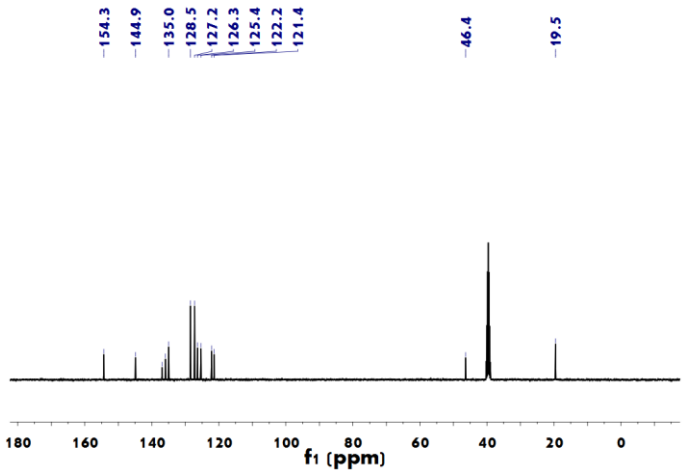

Fig. S21. [13]C NMR spectrum of compound **2A-S** (100 MHz, DMSO-d_6, 298 K).

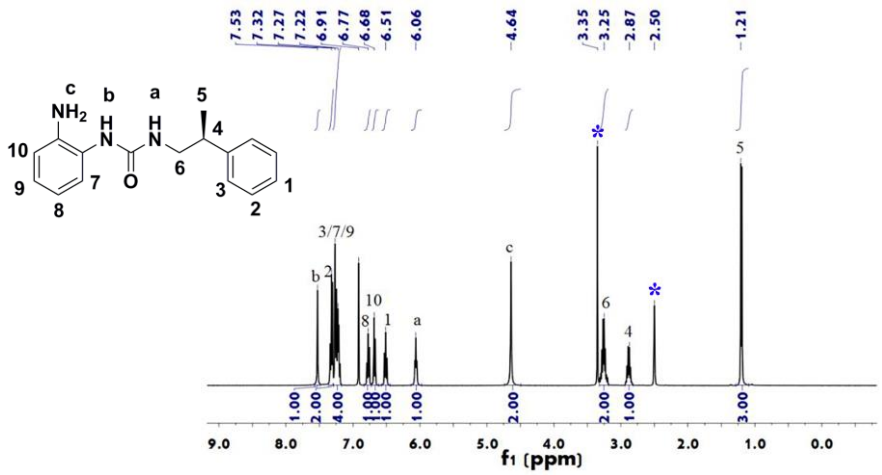

Fig. S22. [1]H NMR spectrum of compound **2B-S** (400 MHz, DMSO-d_6, 298 K).

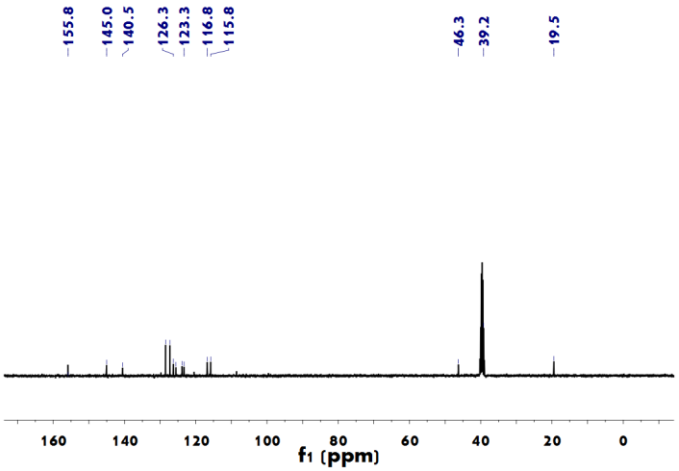

Fig. S23. ^{13}C NMR spectrum of compound **2B-S** (100 MHz, DMSO-d_6, 298 K).

Ligand L^{2S}:

The syntheses of compounds **2A-S** and **2B-S** are similar to those of **2A-R** and **2B-R**, respectively.

Compound **2C** (0.10 g, 0.13 mmol) was dissolved in 10 mL THF and the solution was added dropwise into a 10 mL THF solution of **2B-S** (0.12 g, 0.43 mmol) and trimethylamine (200 μL). The mixture was refluxed overnight and the precipitate thus obtained was filtered off and washed with diethyl ether. After dried over in vacuum, a grey white solid **L^{2S}** (0.12 g, 81 %) was obtained. ^{1}H NMR (400 MHz, DMSO-d_6, ppm): δ 8.99 (s, 1H, NHa), 7.95 (s, 1H, NHb), 7.86 (s, 1H, NHc), 7.54 (m, 1H, H3), 7.44 (m, 1H, H6), 7.35 (d, J = 8 Hz, 1H, H2), 7.30 (m, 1H, H11), 7.26 (d, J = 8 Hz, 1H, H10), 7.20 (m, 1H, H12), 6.90 (d, J = 8 Hz, 1H, H1), 6.42 (m, 1H, NHd), 3.27 (m, 2H, H7), 2.91 (m, 1H, H8), 1.21 (d, J = 8 Hz, 3H, H9). ^{13}C NMR (100 MHz, DMSO-d_6, ppm): 156.1, 153.3, 145.1, 142.1, 134.8, 132.0, 131.2, 128.5, 127.3, 126.3, 124.2, 123.8, 123.5, 119.6, 46.4, 39.8, 19.6. ESI-MS: m/z 1177.1034, $[M+H]^+$.

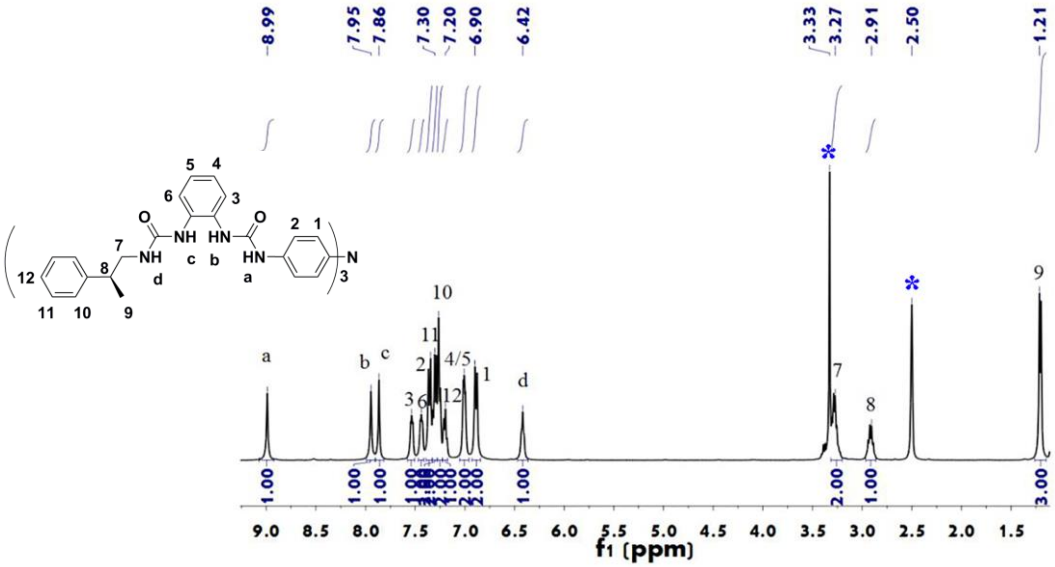

Fig. S24. ^{1}H NMR spectrum of **L^{2S}** (400 MHz, DMSO-d_6, 298 K).

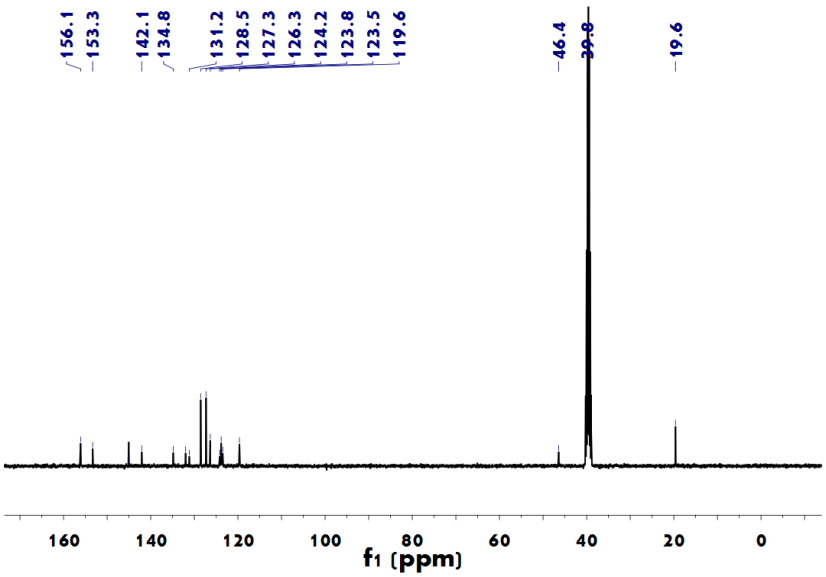

Fig. S25. ^{13}C NMR spectrum of $\mathbf{L^{2S}}$ (100 MHz, DMSO-d_6, 298 K).

S3. Synthesis of complexes and NMR spectroscopy

(TPA)OH (1.37 mg, 0.00675 mmol) and H_3PO_4 (0.259 mg, 0.00265 mmol) were added to a suspension of $\mathbf{L^{1R}/L^{1S}}$ or $\mathbf{L^{2R}/L^{2S}}$ (5 mg) in acetonitrile (1 mL). After stirring overnight at room temperature, a clear light brown solution was obtained. Slow vapor diffusion of diethyl ether into these solutions provided brown crystals. $\mathbf{(TEA)_{12}[(PO_4)_4(L^{Bn})_4]}$ and $\mathbf{(TMA)_{12}[(PO_4)_4(L^{CN})_4]}$ complexes were prepared in a similar way by using $(TEA)_3PO_4$ and $(TMA)_3PO_4$, respectively.

Complex 1 $(TPA)_{12}[(PO_4)_4(\mathbf{L^{1R}})_4]$. ^{1}H NMR (400 MHz, acetone-d_6, ppm): δ 11.86, 11.75 (s, 1H, NHa), 11.09, 10.95 (s, 1H, NHb), 8.93, 8.74 (s, 1H, NHc), 8.19, 8.11 (s, 1H, NHd), 8.03 (m, 2H, H3/6), 7.88 (d, J = 8 Hz, 2H, H2), 7.51 (m, 2H, H10), 7.03 (m, 3H, H9/11), 6.75 (d, J = 8 Hz, 2H, H1), 6.72 (m, 2H, H4/5), 4.94 (m, 1H, H7), 1.43 (m, 3H, H8).

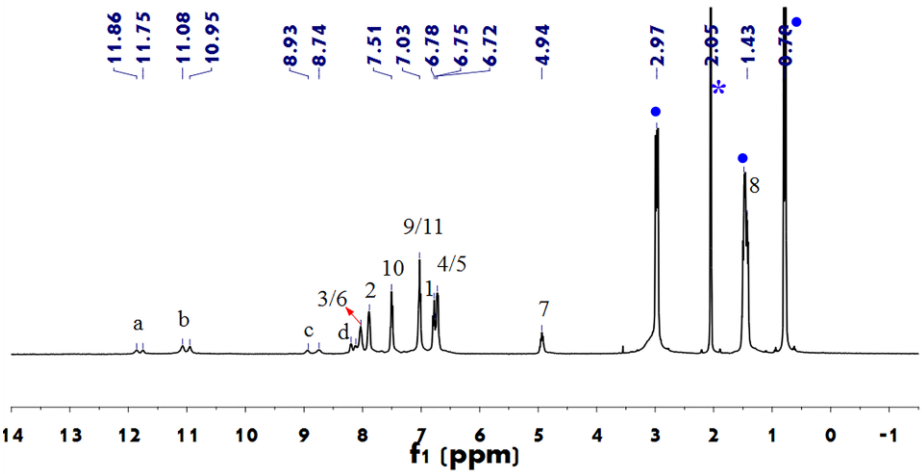

Fig. S26. ^{1}H NMR spectrum of complex $(TPA)_{12}[(PO_4)_4(\mathbf{L^{1R}})_4]$ (**1**) (400 MHz, acetone-d_6, 298 K).

Complex 2 $(TPA)_{12}[(PO_4)_4(\mathbf{L}^{1S})_4]$. ^{1}H NMR (400 MHz, acetone-d_6, ppm): δ 11.74 (s, 1H, NHa), 10.99 10.74 (s, 1H, NHb), 8.93, 8.77 (s, 1H, NHc), 8.19, 8.11 (s, 1H, NHd), 8.03 (m, 2H, H3/6), 7.88 (d, J = 8 Hz, 2H, H2), 7.51 (m, 2H, H10), 7.03 (m, 3H, H9/11), 6.75 (d, J = 8 Hz, 2H, H1), 6.72 (m, 2H, H4/5), 4.94 (m, 1H, H7), 1.43 (m, 3H, H8).

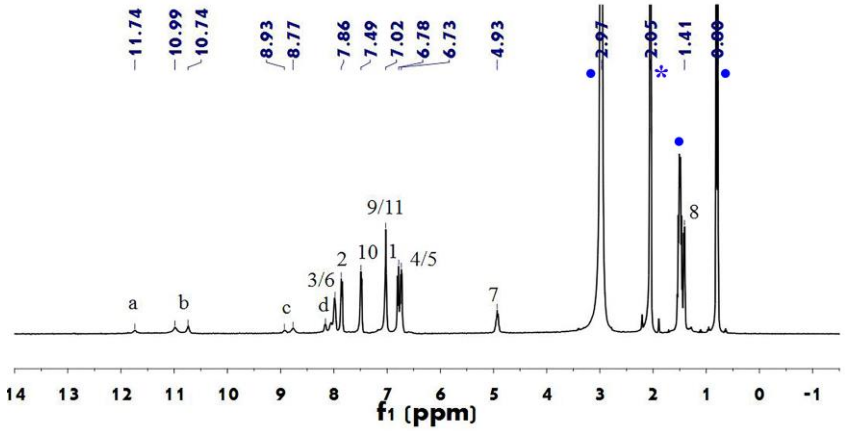

Fig. S27. ^{1}H NMR spectrum of complex $(TPA)_{12}[(PO_4)_4(\mathbf{L}^{1S})_4]$ (**2**) (400 MHz, acetone-d_6, 298 K).

Complex 3 $(TPA)_{12}[(PO_4)_4(\mathbf{L}^{2R})_4]$. ^{1}H NMR (400 MHz, DMSO-d_6, ppm): δ 11.24 (s, 1H, NHb), 11.18 (s, 1H, NHc), 10.90 (s, 1H, NHa), 8.05 (s, 1H, NHd), 7.88 (m, 2H, H3/6), 7.55 (d, J = 8 Hz, 2H, H2), 7.20 (m, 2H, H10), 7.11 (m, 1H, H12), 7.06 (m, 2H, H11), 6.80 (m, 2H, H4/5), 6.61 (d, J = 8 Hz, 2H, H1), 3.16 (m, 1H, H7), 2.85 (m, 3H, H8), 1.07 (m, 1H, H9).

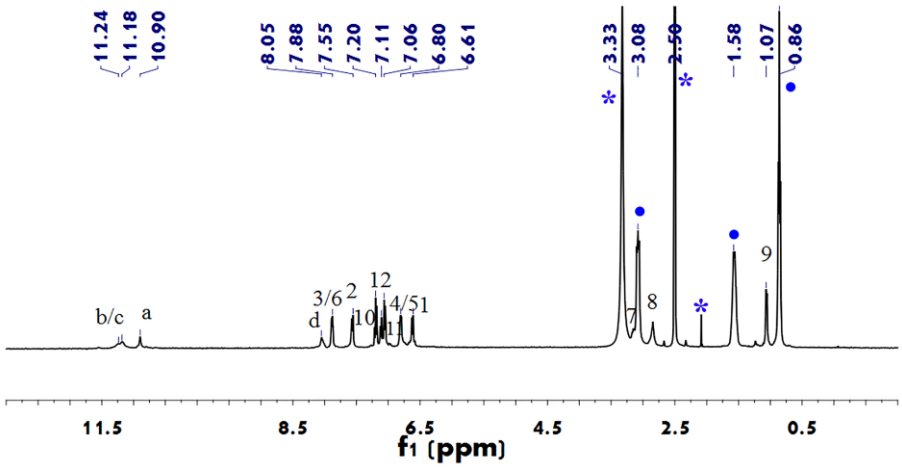

Fig. S28. ^{1}H NMR spectrum of complex $(TPA)_{12}[(PO_4)_4(\mathbf{L}^{2R})_4]$ (**3**) (400 MHz, DMSO-d_6, 298 K).

Complex 4 $(TPA)_{12}[(PO_4)_4(\mathbf{L}^{2S})_4]$. ^{1}H NMR (400 MHz, DMSO-d_6, ppm): δ 11.20 (2H, NHb/c), 10.83 (s, 1H, NHa), 8.10 (s, 1H, NHd), 7.88 (m, 2H, H3/6), 7.60 (d, J = 8 Hz, 2H, H2), 7.20 (m, 2H, H10), 7.11 (m, 1H, H12), 7.06 (m, 2H, H11), 6.81 (m, 2H, H4/5), 6.66 (d, J = 8 Hz, 2H, H1), 3.14 (m, 1H, H7), 2.86 (m, 3H, H8), 1.05 (m, 1H, H9).

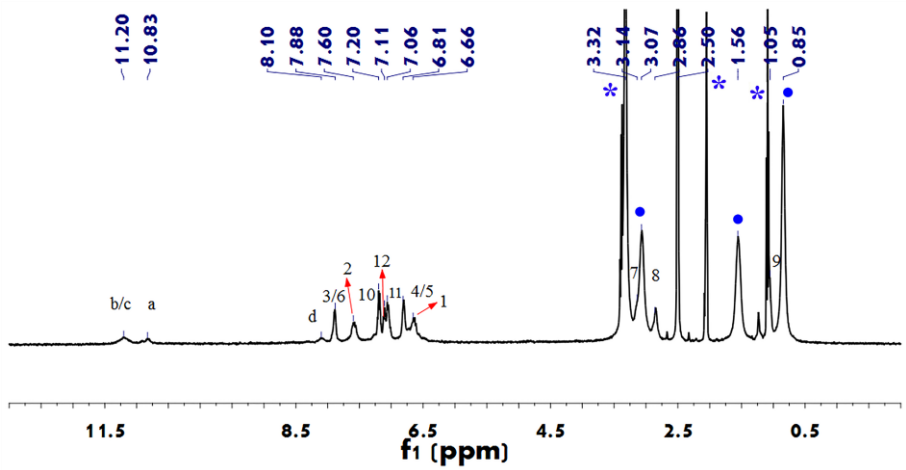

Fig. S29. ^{1}H NMR spectrum of complex $(TPA)_{12}[(PO_4)_4(\mathbf{L}^{2S})_4]$ (**4**) (400 MHz, DMSO-d_6, 298 K).

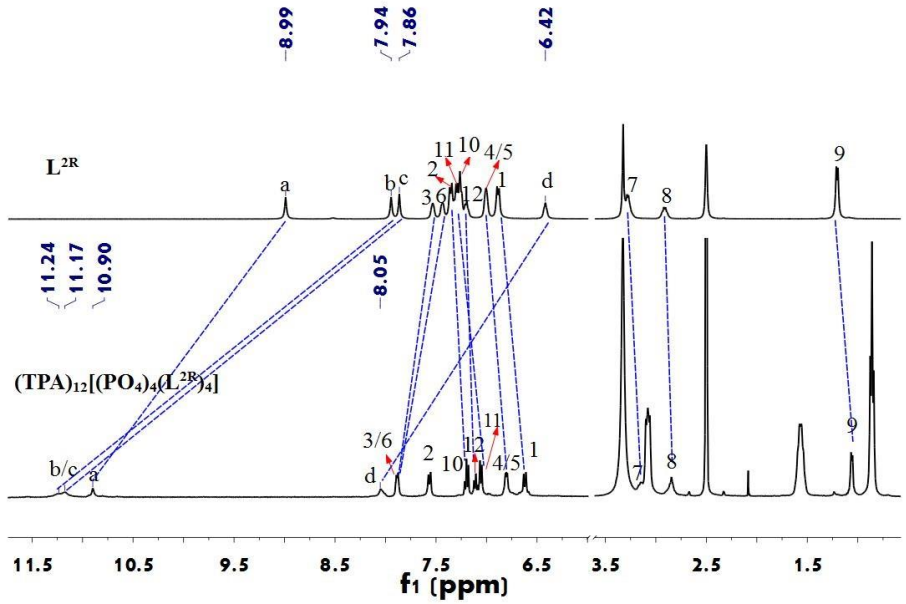

Fig. S30. ^{1}H NMR spectra of complex $(TPA)_{12}[(PO_4)_4(\mathbf{L}^{2R})_4]$ (**3**) and ligand $\mathbf{L}^{2R}$ in DMSO-d_6 (400 MHz, 298 K).

Complex 5 $(TEA)_{12}[(PO_4)_4(\mathbf{L}^{Bn})_4]$. ^{1}H NMR (400 MHz, CD_3CN, ppm): δ 13.26 (s, 1H, NHa), 11.62 (s, 1H, NHb), 11.03 (s, 1H, NHc), 10.55 (s, 1H, NHd), 7.89 (m, 4H, H2/3/6), 7.09 (m, 1H, H10), 7.13 (m, 4H, H8/9), 6.77 (m, 2H, H4/5), 6.54 (d, J = 8 Hz, 2H, H1), 3.83 (d, J = 8 Hz, 2H, H7).

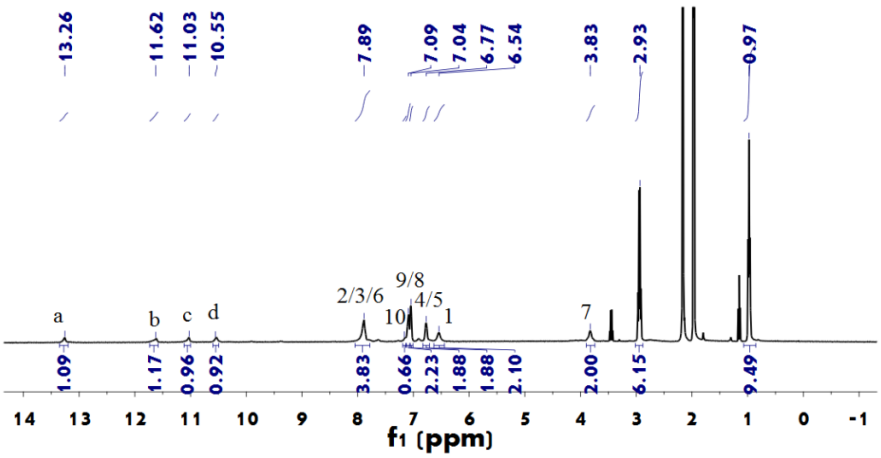

Fig. S31. ^{1}H NMR spectrum of complex $(TEA)_{12}[(PO_4)_4(\mathbf{L}^{Bn})_4]$ (**5**) (400 MHz, CD_3CN, 298 K).

Complex 6 $(TMA)_{12}[(PO_4)_4(\mathbf{L}^{CN})_4]$ ^{1}H NMR (400 MHz, acetone-d_6, ppm): δ 12.68 (s, 1H, NHd), 12.17 (s, 1H, NHc), 12.04 (s, 2H, NHb/a), 8.25 (m, 1H, H6), 8.04 (m, 1H, H3), 7.76 (m, 2H, H7), 7.44 (d, J = 8 Hz, 2H, H2), 6.88 (m, 4H, H4/5/8), 6.53 (d, J = 8 Hz, 2H, H1).

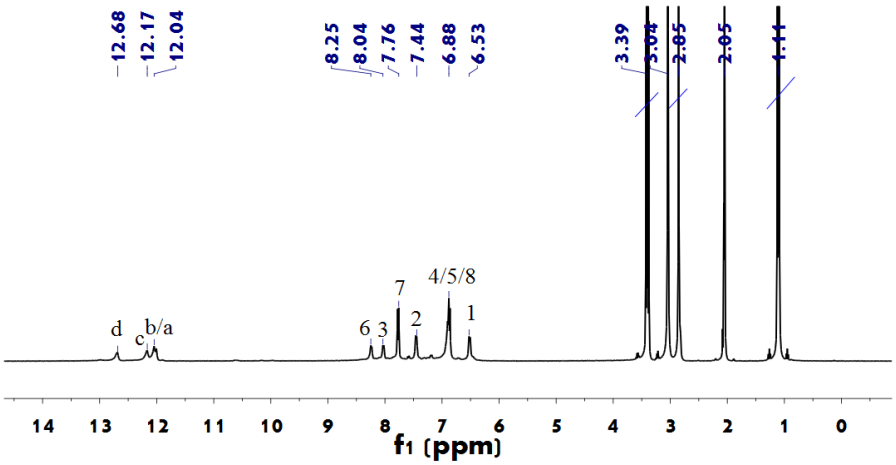

Fig. S32. ^{1}H NMR spectrum of complex $(TMA)_{12}[(PO_4)_4(\mathbf{L}^{CN})_4]$ (**6**) (400 MHz, acetone-d_6, 298 K).

S4. COSY and DOSY spectroscopy

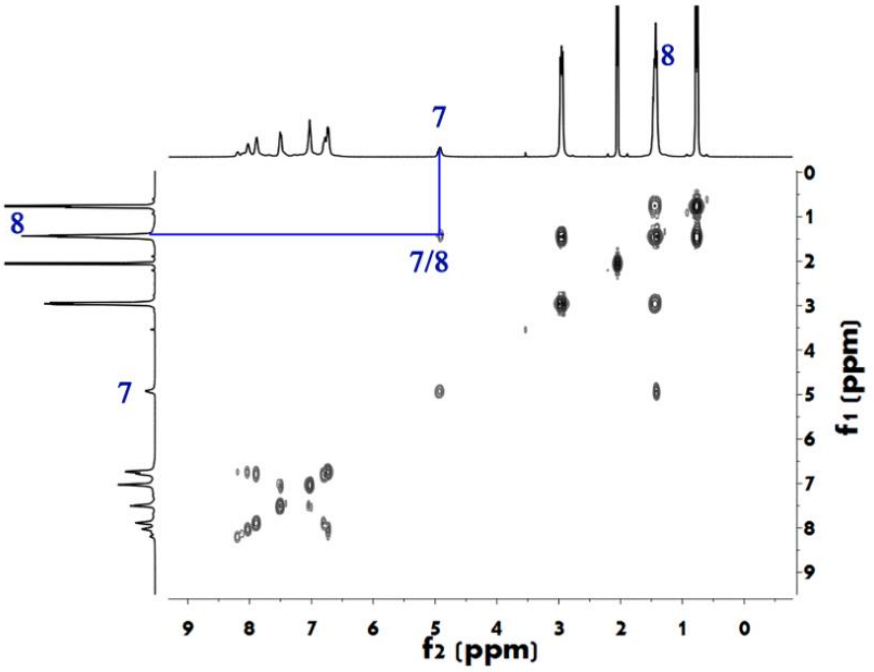

Fig. S33. Partial ^{1}H-^{1}H COSY spectrum of $(TPA)_{12}[(PO_4)_4(\mathbf{L^{1R}})_4]$ (**1**) (400 MHz, acetone-d_6, 298 K).

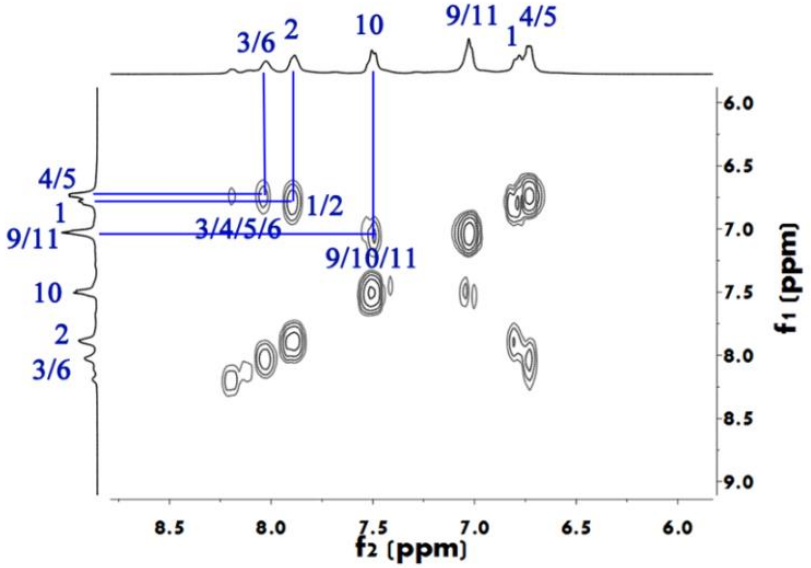

Fig. S34. Aromatic-region ^{1}H-^{1}H COSY spectrum of $(TPA)_{12}[(PO_4)_4(\mathbf{L^{1R}})_4]$ (**1**) (400 MHz, acetone-d_6, 298 K).

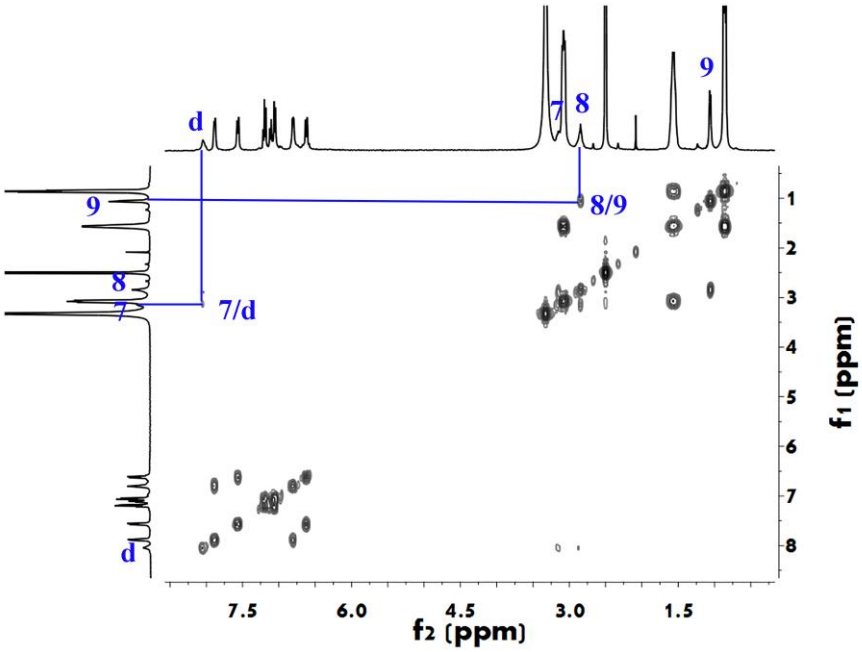

Fig. S35. Partial ^{1}H-^{1}H COSY spectrum of $(TPA)_{12}[(PO_4)_4(\mathbf{L}^{2R})_4]$ (**3**) (400 MHz, DMSO-d_6, 298 K).

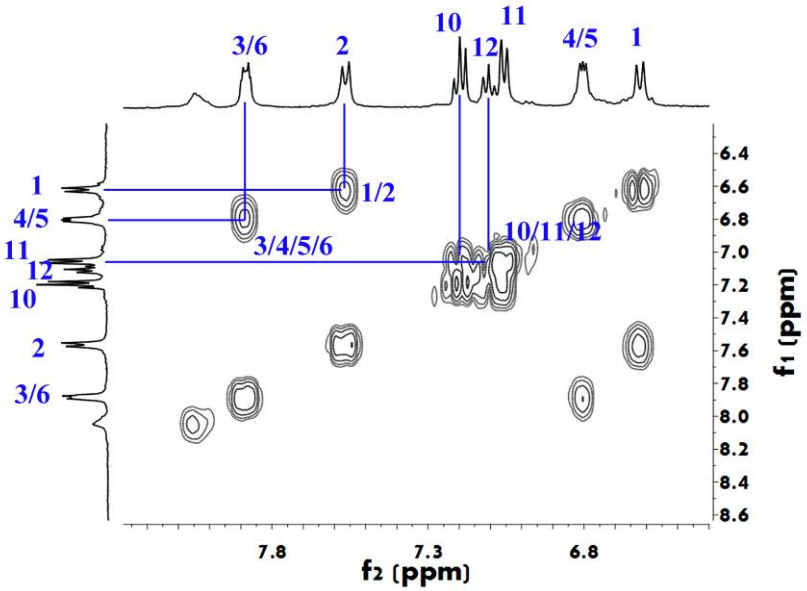

Fig. S36. Aromatic-region ^{1}H-^{1}H COSY spectrum of $(TPA)_{12}[(PO_4)_4(\mathbf{L}^{2R})_4]$ (**3**) (400 MHz, DMSO-d_6, 298 K).

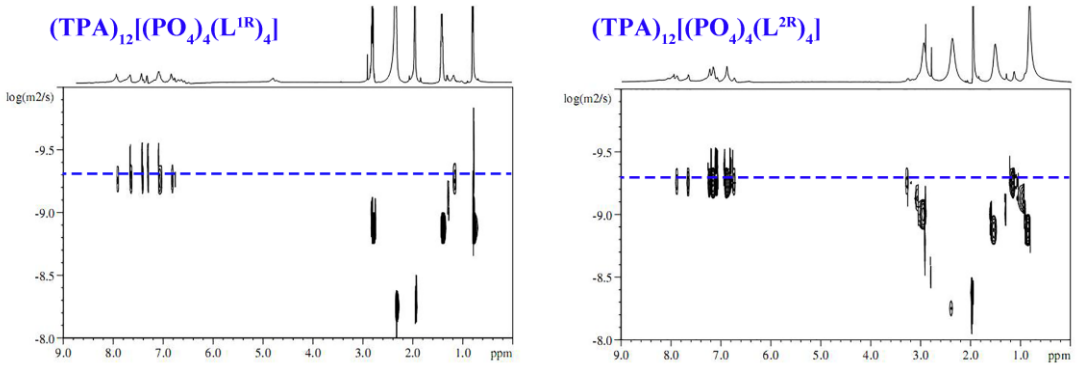

Fig. S37. DOSY spectra of $(TPA)_{12}[(PO_4)_4(\mathbf{L^{1R}})_4]$ (**1**) and $(TPA)_{12}[(PO_4)_4(\mathbf{L^{2R}})_4]$ (**3**) (400 MHz, CD_3CN, 298 K).

S5. High-resolution MS studies

The complexes were dissolved in acetonitrile (c = 0.5 mg/mL) and measured by direct infusion with negative polarity, dry gas 4.0 L/min at 180 ℃, nebulizer gas 0.4 bar, capillary voltage 4500 V and end plate offset –500 V.

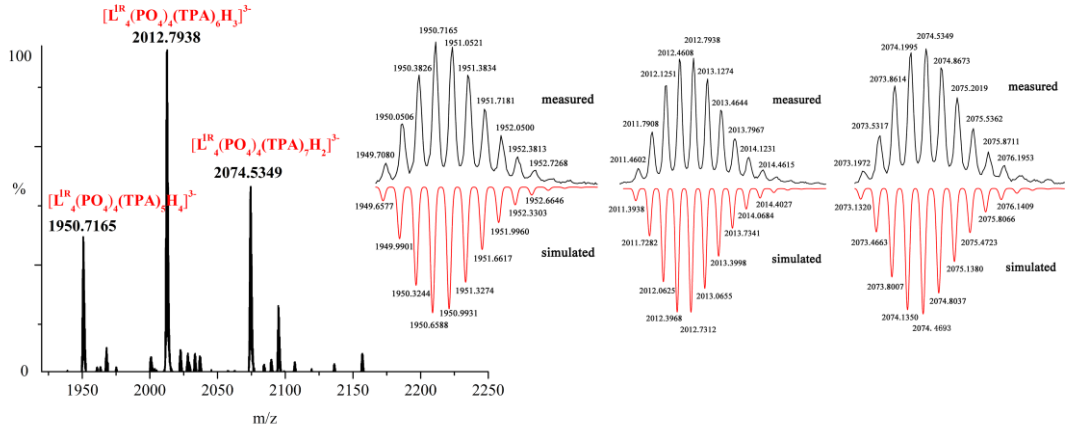

Fig. S38. High-resolution ESI-mass spectrum of $(TPA)_{12}[(PO_4)_4(\mathbf{L^{1R}})_4]$ (complex **1**).

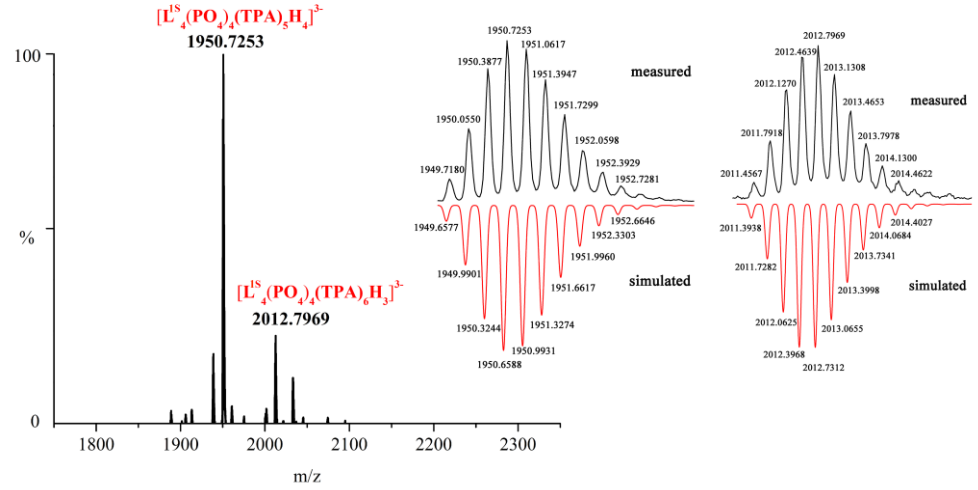

Fig. S39. High-resolution ESI-mass spectrum of $(TPA)_{12}[(PO_4)_4(\mathbf{L^{1S}})_4]$ (**2**).

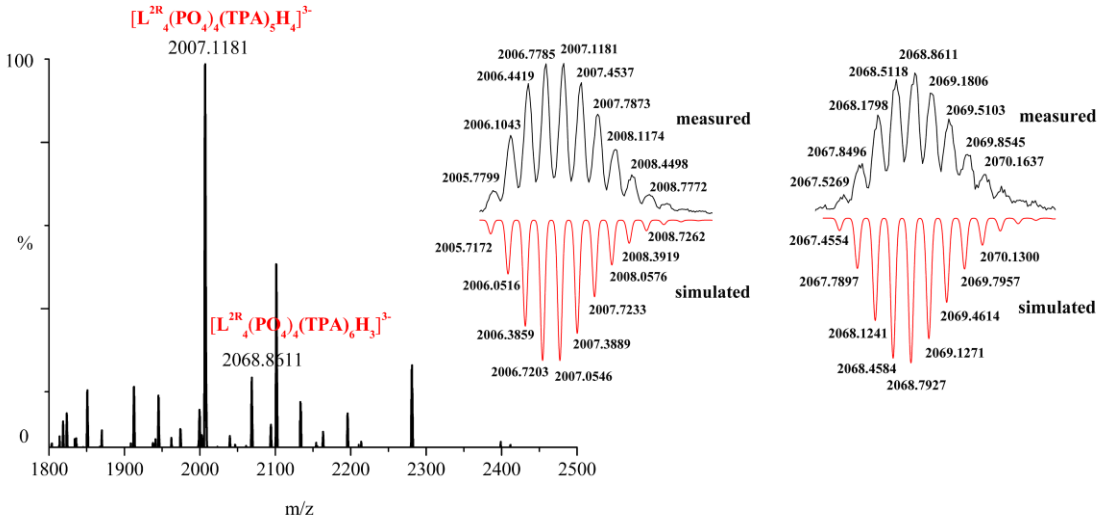

Fig. S40. High-resolution ESI-mass spectrum of $(TPA)_{12}[(PO_4)_4(\mathbf{L^{2R}})_4]$ (**3**).

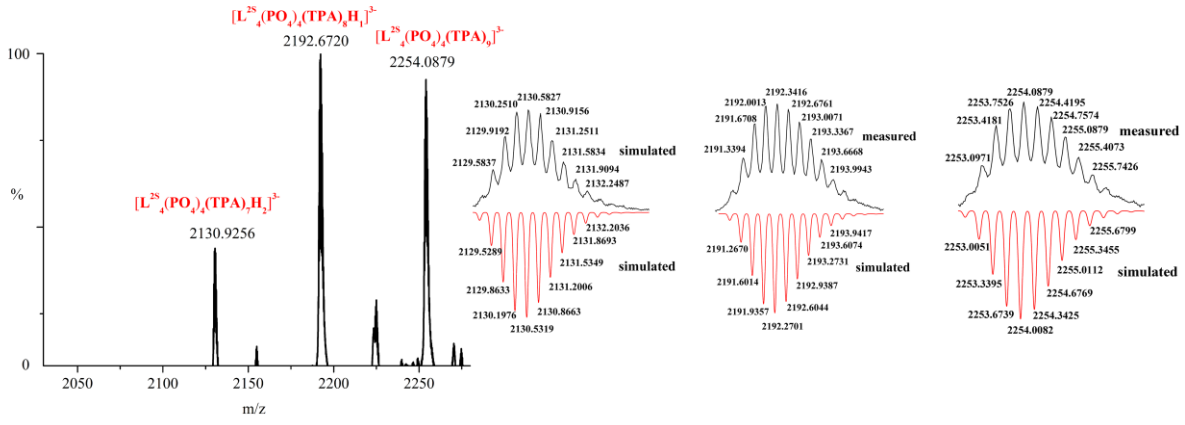

Fig. S41. High-resolution ESI-mass spectrum of $(TPA)_{12}[(PO_4)_4(\mathbf{L^{2S}})_4]$ (**4**).

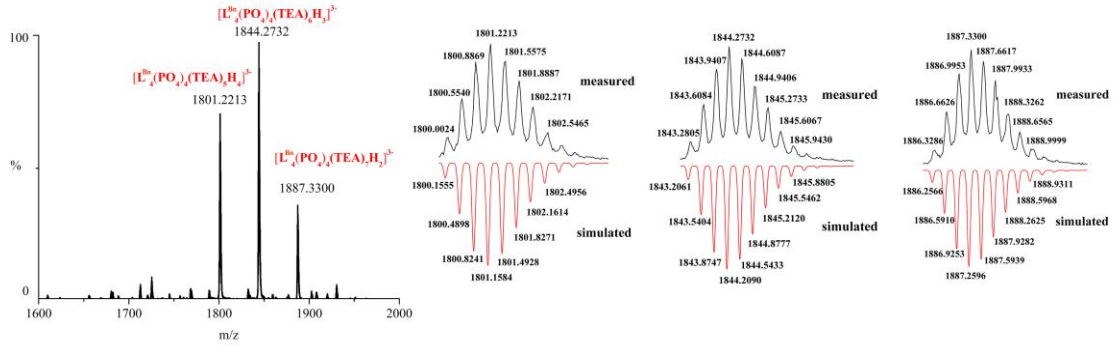

Fig. S42. High-resolution ESI-mass spectrum of $(TEA)_{12}[(PO_4)_4(\mathbf{L}^{\mathbf{Bn}})_4]$ (**5**).

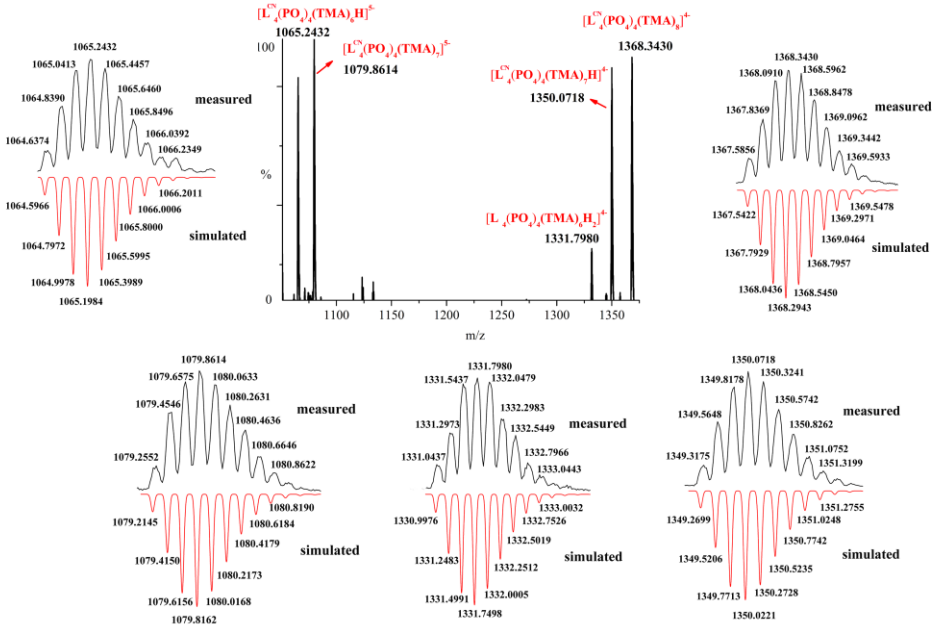

Fig. S43. High-resolution ESI-mass spectrum of $(TMA)_{12}[(PO_4)_4(\mathbf{L}^{\mathbf{CN}})_4]$ (**6**).

S6. X-ray crystallography of complexes 1, 2 and 5

Diffraction data for the complexes **1**, **2** and **5** were performed on a Bruker D8 Venture photon II, at low temperature (120 K) with Cu-K radiation (λ = 1.54178 Å). An empirical absorption correction using SADABS was applied for all data.[3] All structures were solved and refined to convergence on F^2 for all independent reflections by the full-matrix least squares method using the OLEX2 1.2.[4]

In complex **1**, there are additional, severely disordered cations and solvent molecules in the crystal lattice (about one TPA^+ and eight H_2O molecules per formula, Z = 4), approximately 748 electron equivalents were removed from the unit cell using the SQUEEZE routine implemented within the software program PLATON,[5] and the resulting .fab file was processed using the ABIN instruction. In this structure, as it was not possible to see clear electron-density peaks in difference maps which would correspond with acceptable locations for the O22 water H atoms, the refinement was completed with no allowance for these water H atoms in the model.

In complex **2**, there are additional, severely disordered molecules in the crystal lattice (about one TPA, one MeCN and six H_2O molecules per formula, Z = 4), and the SQUEEZE command was employed in the refinement of the structure. Approximately 768 electron equivalents were removed from unit cell.

In complex **5**, there are additional, severely disordered solvent molecules in the crystal lattice (about one MeCN and one H_2O per formula, Z = 8), and the SQUEEZE command was employed in the refinement of the structure. Approximately 263 electron equivalents were removed from unit cell.

Crystallographic data and refinement details for **1**, **2** and **5** are given in Table S4. CCDC 1955042 for $(TPA)_{12}[(PO_4)_4(\mathbf{L}^{\mathbf{1R}})_4]$•MeCN•$H_2O$ (**1**), 1957114 for $(TPA)_{12}[(PO_4)_4(\mathbf{L}^{\mathbf{1S}})_4]$ (**2**) and 1955280 for $(TEA)_{12}[(PO_4)_4(\mathbf{L}^{\mathbf{Bn}})_4]$ (**5**). These data can be obtained free of charge from the Cambridge Crystallographic Data Centre www.ccdc.cam.ac.uk/data_request/cif.

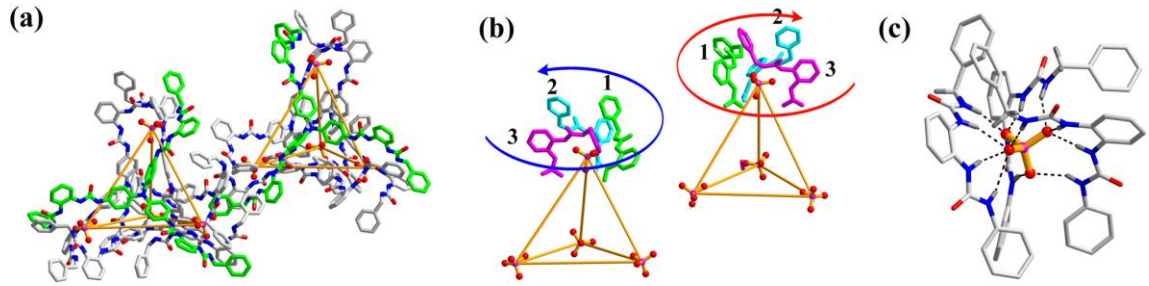

Fig. S44. (a) Crystal structure of $(TEA)_{12}[(PO_4)_4(\mathbf{L}^{\mathbf{Bn}})_4]$ (**5**) (ΔΔΔΔ and ΛΛΛΛ isomers in the same cell); (b) Δ or Λ configuration at the vertices; (c) hydrogen bonds around PO_4^{3-} (N ··O distances range from 2.62 to 3.08 Å; N−H ··O angles range from 132 to 176°). All TEA^+ ions and hydrogens (without the NH ones) were omitted for clarity.

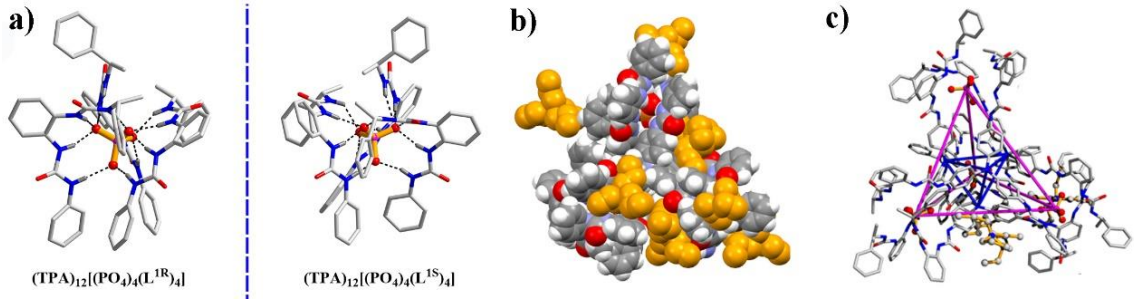

Fig. S45. (a) Hydrogen bonds around PO_4^{3-}; (b) typical TPA cations (yellow) in the crystal of $(TPA)_{12}[(PO_4)_4(\mathbf{L}^{\mathbf{1R}})_4]$ (the rest TPA cations were omitted for clarity). TPA cations in the crystal structure are found outside the cage and all of them are located very close to the tetrahedron, either in the grooves formed by adjacent ligands or around the vertices. (c) The tetrahedral cavity formed by the chiral ligands $\mathbf{L}^{\mathbf{1R/1S}}$ is distorted, stretching in one direction, where the PO_4 ··PO_4 separations range from about 13.6 Å to 15.3 Å (magenta, right), and the N ··N separation between every ligand is from 5.84 Å to 6.56 Å (blue, right).

Table S1. Hydrogen bonds of complex $(TPA)_{12}[(PO_4)_4(\mathbf{L}^{1R})_4]$•MeCN•$H_2O$ (**1**).

D–H···A	Symmetry Operation	d(D–H) (Å)	d(H···A) (Å)	d(D···A) (Å)	∠(DHA) (°)
N2–H2A···O16	-x+1, y, -z+1	0.88	1.98	2.825(5)	162
N3–H3A···O15	-x+1, y, -z+1	0.88	1.89	2.726(7)	157
N4–H4···O15	-x+1, y, -z+1	0.88	1.99	2.813(6)	154
N5–H5A···O14	-x+1, y, -z+1	0.88	1.99	2.813(7)	156
N6–H6A···O16		0.88	2.08	2.894(5)	153
N7–H7···O14		0.88	1.84	2.702(6)	166
N8–H8···O14		0.88	1.84	2.709(7)	167
N9–H9A···O13		0.88	2.12	2.820(6)	136
N10–H10A···O18	-x+1, y, -z+1	0.88	1.94	2.819(6)	179
N11–H11A···O19	-x+1, y, -z+1	0.88	1.93	2.767(7)	160
N12–H12A···O19	-x+1, y, -z+1	0.88	1.97	2.821(8)	162
N13–H13···O17	-x+1, y, -z+1	0.88	1.98	2.857(8)	172
N15–H15A···O20	-x+1, y, -z+1	0.88	1.92	2.746(6)	155
N16–H16···O20	-x+1, y, -z+1	0.88	1.93	2.747(7)	154
N17–H17···O19	-x+1, y, -z+1	0.88	2.15	2.966(7)	154
N18–H18A···O19	-x+1, y, -z+1	0.88	2.16	2.964(6)	152
N19–H19A···O13		0.88	1.94	2.771(5)	158
N20–H20A···O13		0.88	2.02	2.823(4)	151
N21–H21A···O15		0.88	1.94	2.784(6)	159
N22–H22A···O15		0.88	2.26	3.020(7)	145
N23–H23···O18		0.88	2.04	2.871(5)	157
N24–H24A···O17		0.88	1.83	2.700(5)	170
N25–H25A···O17		0.88	1.85	2.717(8)	169
N26–H26···O20		0.88	2.03	2.865(8)	157

Table S2. Hydrogen bonds of complex $(TPA)_{12}[(PO_4)_4(\mathbf{L}^{1S})_4]$ (**2**).

D–H···A	Symmetry Operation	d(D–H) (Å)	d(H···A) (Å)	d(D···A) (Å)	∠(DHA) (°)
N2–H2A···O18	-x+1, y, -z+1	0.88	1.95	2.786(9)	160
N3–H3A···O17	-x+1, y, -z+1	0.88	1.89	2.745(10)	164
N4–H4···O17	-x+1, y, -z+1	0.88	1.99	2.815(10)	155
N5–H5A···O20	-x+1, y, -z+1	0.88	1.98	2.808(12)	157
N6–H6A···O18		0.88	2.09	2.906(8)	153
N7–H7···O20		0.88	1.86	2.727(9)	166
N8–H8···O20		0.88	1.86	2.733(10)	169
N9–H9A···O19		0.88	2.15	2.836(10)	135
N10–H10A···O14		0.88	1.95	2.831(9)	178
N11–H11A···O13		0.88	1.96	2.814(12)	165
N12–H12A···O13		0.88	1.97	2.815(16)	161
N13–H13···O15		0.88	1.94	2.818(19)	173
N15–H15A···O14	-x+1, y, -z+1	0.88	2.04	2.867(8)	157
N16–H16···O15	-x+1, y, -z+1	0.88	1.82	2.701(13)	175
N17–H17···O15	-x+1, y, -z+1	0.88	1.87	2.73(2)	169
N18–H18A···O16	-x+1, y, -z+1	0.88	2.02	2.870(14)	163
N19–H19A···O16		0.88	1.92	2.732(10)	153
N20–H20A···O16		0.88	1.92	2.737(11)	154
N21–H21A···O13		0.88	2.15	2.962(12)	154
N22–H22A···O13		0.88	2.20	3.000(10)	151
N23–H23···O19		0.88	1.93	2.765(8)	157
N24–H24A···O19		0.88	2.00	2.807(7)	152
N25–H25A···O17		0.88	1.94	2.776(10)	159
N26–H26···O17		0.88	2.27	3.036(12)	145

Table S3. Hydrogen bonds of complex $(TEA)_{12}[(PO_4)_4(\mathbf{L}^{Bn})_4]$ (**5**).

D–H···A	Symmetry Operation	d(D–H) (Å)	d(H···A) (Å)	d(D···A) (Å)	∠(DHA) (°)
N2–H2A···O10	-x+1, y, -z+1/2	0.88	2.01	2.872(4)	165
N3–H3A···O7	-x+1, y, -z+1/2	0.88	1.83	2.699(5)	169
N4–H4···O7	-x+1, y, -z+1/2	0.88	1.90	2.752(5)	164
N5–H5A···O9	-x+1, y, -z+1/2	0.88	1.98	2.790(4)	153
N6–H6A···O10	x, -y, -z+1/2	0.88	2.06	2.854(4)	150
N7–H7···O9	x, -y, -z+1/2	0.88	1.86	2.742(4)	175
N8–H8···O9	x, -y, -z+1/2	0.88	1.90	2.770(4)	172
N9–H9A···O8	x, -y, -z+1/2	0.88	1.90	2.769(6)	169
N10–H10A···O8		0.88	2.41	3.082(5)	133
N11–H11A···O8		0.88	1.84	2.631(6)	149
N12–H12A···O8		0.88	2.14	2.987(5)	162
N13–H13···O7		0.88	1.91	2.777(6)	167

Table S4. Crystal data and refinement details for complexes **1**, **2** and **5**.

	Complex **1** $(TPA)_{12}[(PO_4)_4(\mathbf{L}^{1R})_4]$•MeCN•$H_2O$	Complex **2** $(TPA)_{12}[(PO_4)_4(\mathbf{L}^{1S})_4]$	Complex **5** $(TEA)_{12}[(PO_4)_4(\mathbf{L}^{Bn})_4]$
Empirical formula	$C_{206}H_{299}N_{33}O_{21}P_2$	$C_{204}H_{294}N_{32}O_{20}P_2$	$C_{87}H_{117}N_{16}O_{10}P_1$
Formula weight	3635.70	3576.63	1577.93
Crystal system	Monoclinic	Monoclinic	Tetragonal
space group	C_2	C_2	P-4 2c
a (Å)	40.8647(13)	40.912(5)	25.958(3)
b (Å)	28.7021(9)	28.685(5)	25.958(3)
c (Å)	26.5738(9)	26.497(5)	28.548(8)
α (deg)	90	90	90
β (deg)	129.6000(10)	129.742(12)	90
γ (deg)	90	90	90
V (Å^3)	24015.7(14)	23911(8)	19236(7)
T (K)	120(2)	120(2)	158(2)
Z	4	4	8

D_{calc} (g·cm^{-3})	1.043	1.035	1.130
Total no. of data	140177	169372	366390
No. of unique data	43237	39020	35354
θ range (deg)	2.266-68.256	2.192-63.968	3.53-68.03
Completeness to θ	99.8%	97.3%	99.6%
Goodness-of-fit on F^2	1.072	1.112	1.031
R(int)	0.0688	0.1009	0.0447
$R1$ [$I>2\sigma(I)$]	0.0958	0.0923	0.0674
$wR2$ [$I>2\sigma(I)$]	0.2211	0.2070	0.1941

S7. CD spectroscopy

Ligands were dissolved in DMSO:CH_3CN = 1:99 (c = 4×10^{-5} mol/L) and the complexes were dissolved in CH_3CN (c = 4×10^{-5} mol/L, calculated by ligand).

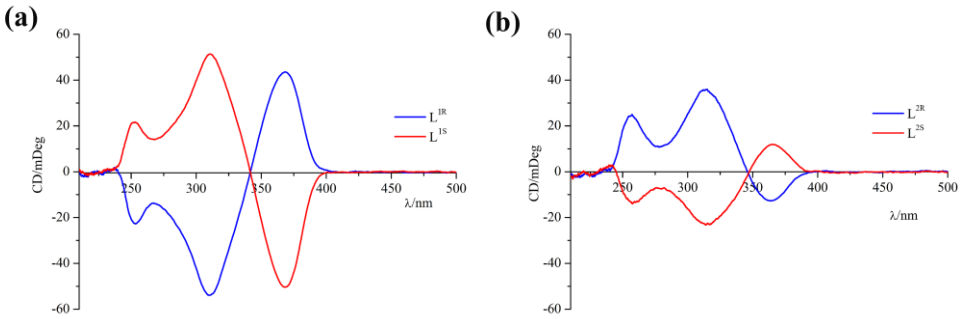

Fig. S46. CD spectra (a) **L$^{1R/1S}$**; (b) **L$^{2R/2S}$** in DMSO:CH_3CN = 1:99 (c = 4×10^{-5} mol/L).

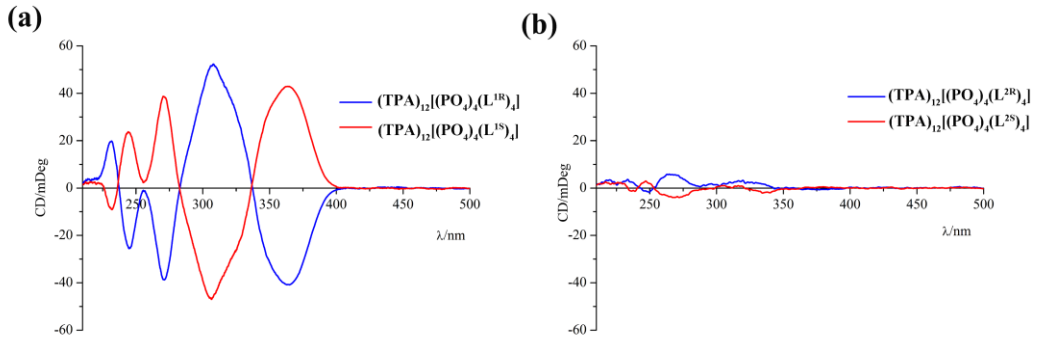

Fig. S47. CD spectra (a) $(TPA)_{12}[(PO_4)_4(\mathbf{L}^{1R/1S})_4]$; (b) $(TPA)_{12}[(PO_4)_4(\mathbf{L}^{2R/2S})_4]$ in CH_3CN (c = 4×10^{-5} mol/L, calculated by ligand).

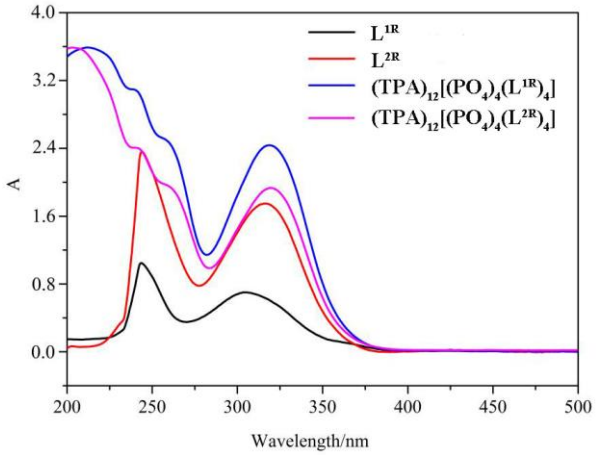

Fig. S48. UV-vis comparison of ligands $\mathbf{L^{1R}}$, $\mathbf{L^{2R}}$, and complexes $(TPA)_{12}[(PO_4)_4(\mathbf{L^{1R}})_4]$ (**1**) and $(TPA)_{12}[(PO_4)_4(\mathbf{L^{2R}})_4]$ (**3**) (c = 4×10^{-5} mol/L, calculated by ligand).

S8. Chirality transcription in chiral-achiral mixed-ligand systems

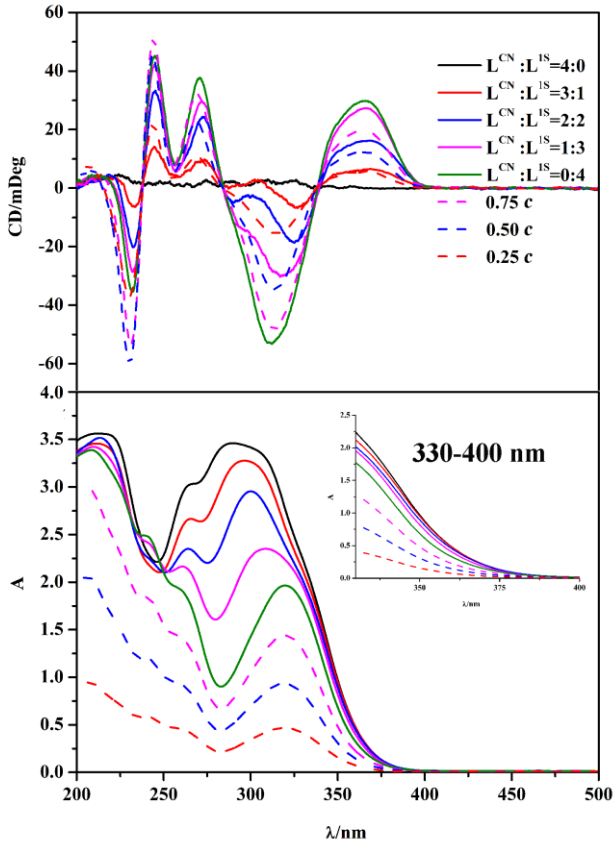

Fig. S49. CD and UV-vis spectra of $(TPA)_{12}[(PO_4)_4(\mathbf{L^{CN}})_{4-n}(\mathbf{L^{1S}})_n]$ (n = 0−4) (solid lines) and gradually diluted $(TPA)_{12}[(PO_4)_4(\mathbf{L^{1S}})_4]$ solution (from c = 4×10^{-5} mol/L to 0.75c, 0.50c and 0.25c, calculated by ligand) (dash lines).

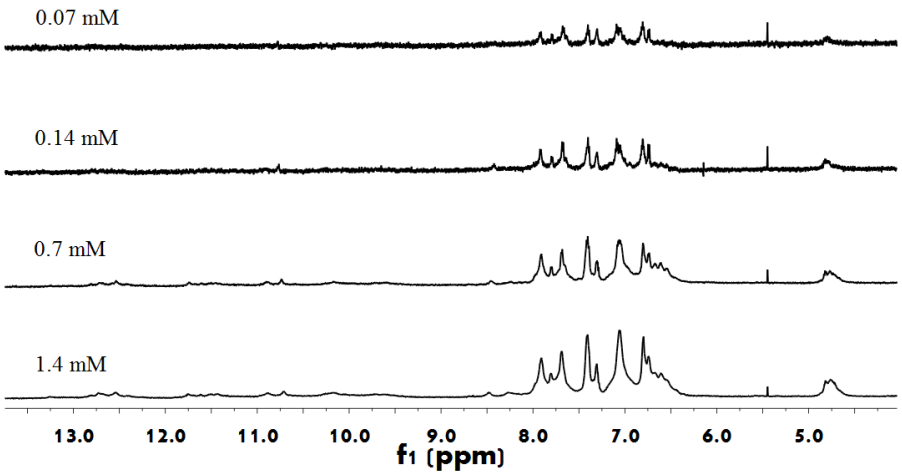

Fig. S50. ^{1}H NMR spectra of gradually diluted $(TPA)_{12}[(PO_4)_4(\mathbf{L}^{\mathbf{1S}})_4]$ (400 MHz, CD_3CN, 298 K).

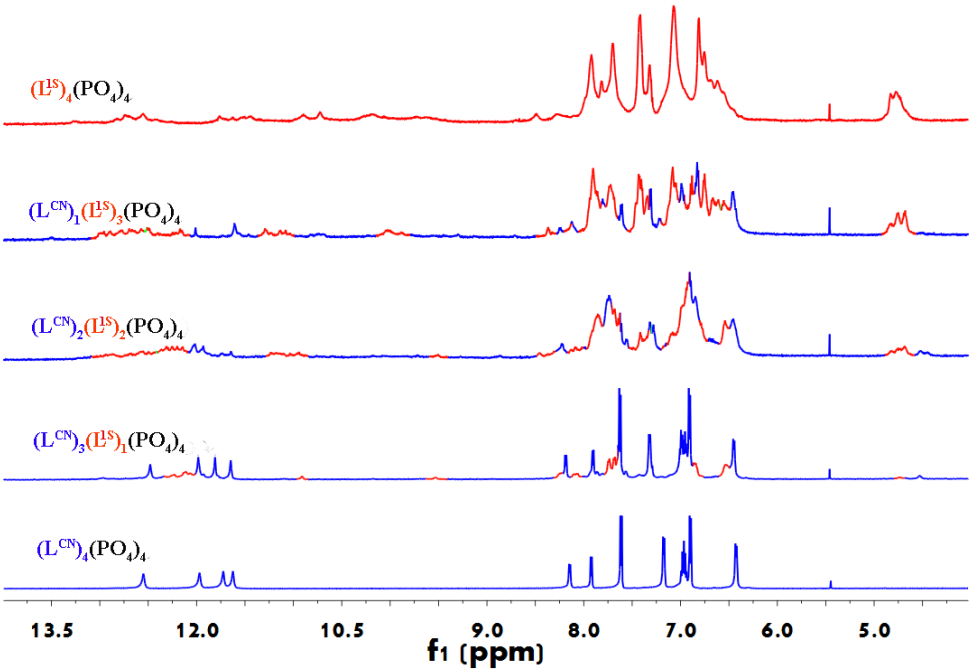

Fig. S51. ^{1}H NMR spectra of $(TPA)_{12}[(PO_4)_4(\mathbf{L}^{\mathbf{CN}})_{4-n}(\mathbf{L}^{\mathbf{1S}})_n]$ (400 MHz, CD_3CN, 298 K).

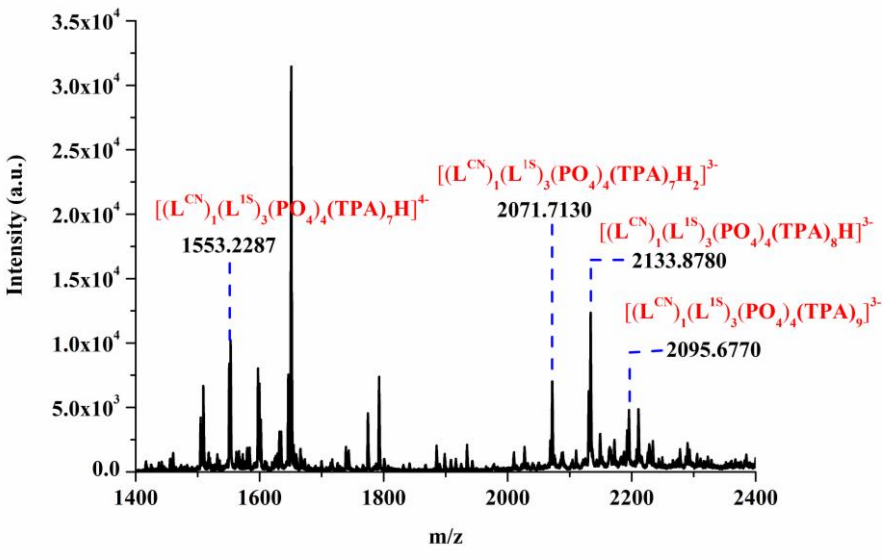

Fig. S52. ESI-MS spectrum of $(TPA)_{12}[(PO_4)_4(\mathbf{L}^{CN})_1(\mathbf{L}^{1S})_3]$.

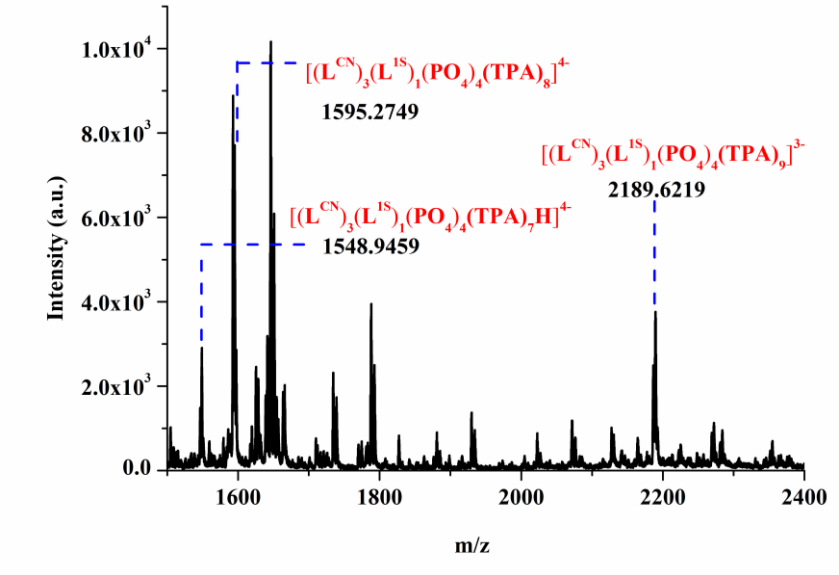

Fig. S53. ESI-MS spectrum of $(TPA)_{12}[(PO_4)_4(\mathbf{L}^{CN})_3(\mathbf{L}^{1S})_1]$.

References:

1. B. Wu, F. Cui, Y. Lei, S. Li, N. d. S. Amadeu, C. Janiak, Y. J. Lin, L. H. Weng, Y. Y. Wang and X. J. Yang, *Angew. Chem. Int. Ed.*, 2013, **52**, 5096–5100.
2. J. Zhao, D. Yang, Y. Zhao, L. Cao, Z. Zhang, X.-J. Yang and B. Wu, *Dalton Trans.*, 2016, **45**, 7360–7365.
3. G. M. Sheldrick, Program SADABS: Area-Detector Absorption Correction, **1996**, University of Göttingen, Germany.
4. O. V. Dolomanov, L. J. Bourhis, R. J. Gildea, J. A. K. Howard and H. Puschmann, *J. Appl. Cryst.* **2009**, *42*, 339–341.
5. A. L. Spek, *Acta Cryst.* **2015**, *C71*, 9–18.